



저작자표시-비영리-변경금지 2.0 대한민국

이용자는 아래의 조건을 따르는 경우에 한하여 자유롭게

- 이 저작물을 복제, 배포, 전송, 전시, 공연 및 방송할 수 있습니다.

다음과 같은 조건을 따라야 합니다:



저작자표시. 귀하는 원저작자를 표시하여야 합니다.



비영리. 귀하는 이 저작물을 영리 목적으로 이용할 수 없습니다.



변경금지. 귀하는 이 저작물을 개작, 변형 또는 가공할 수 없습니다.

- 귀하는, 이 저작물의 재이용이나 배포의 경우, 이 저작물에 적용된 이용허락조건을 명확하게 나타내어야 합니다.
- 저작권자로부터 별도의 허가를 받으면 이러한 조건들은 적용되지 않습니다.

저작권법에 따른 이용자의 권리는 위의 내용에 의하여 영향을 받지 않습니다.

이것은 [이용허락규약\(Legal Code\)](#)을 이해하기 쉽게 요약한 것입니다.

[Disclaimer](#)

**Magnetic nanoparticles control  
neural stem cell behavior in  
normal and ischemic brain**



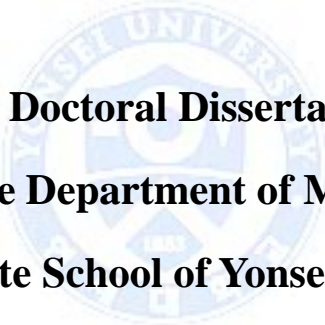
**Seokhwan Yun**

**Department of Medical Science**

**The Graduate School, Yonsei University**

**Magnetic nanoparticles control  
neural stem cell behavior in  
normal and ischemic brain**

**Directed by Professor Kook In Park**



**The Doctoral Dissertation  
submitted to the Department of Medical Science,  
the Graduate School of Yonsei University  
in partial fulfillment of the requirements for the  
degree of Doctor of Philosophy**

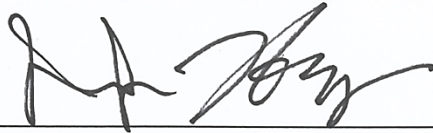
**Seokhwan Yun**

**December 2015**

**This certifies that the Doctoral  
Dissertation of Seokhwan Yun is approved.**



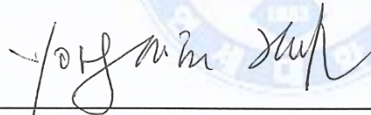
Thesis Supervisor: Kook In Park



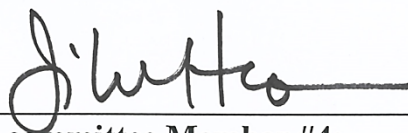
Thesis committee Member #1: Jae-Hyung Jang



Thesis committee Member #2: Joon Soo Lee



Thesis committee Member #3: Yong-Min Huh



Thesis committee Member #4: Ji Hoe Heo

**The Graduate School  
Yonsei University  
December 2015**

## ACKNOWLEDGEMENTS

Today, I am really pleased to get my Doctoral degree with numerous assistance.

I give thanks for financial support from BK21 project, especially graduated school tuition and cost to attend the international association annual meeting. In addition, I also give thanks to Ministry of Future creation and Science which supplied the enriched research grant, and Yonsei medical research center which supplied the laboratory and experimental equipment.

I especially wish to express my sincere gratitude to my supervisor, Great professor Kook In Park, who has given me advise, guidance, and encouragement throughout my doctoral course and made this dissertation possible.

I would also like to record my appreciation to professor Jae-Hyung Jang, Joon Soo Lee, Yong-Min Huh, and Ji Hoe Heo for their valuable suggestions and strict advisement on this dissertation.

Thanks are also due to lab colleagues for their assistance and useful suggestions in preparing this manuscript.

As always, my family has been there, providing emotional and financial support.

## TABLE OF CONTENTS

<b>ABSTRACT</b> .....	1
<b>I. INTRODUCTION</b> .....	2
<b>II. MATERIALS AND METHODS</b> .....	5
1. Culture of human neural stem cells .....	5
2. Firefly luciferase expressing neural stem cells .....	6
3. Synthesis of Zn-doped magnetic nanoparticle .....	6
4. Intracellular labeling of Zn-doped magnetic nanoparticle into neural stem cells .....	8
5. Magnet guided cell delivery <i>in vitro</i> and <i>in vivo</i> .....	9
6. Cytotoxicity of Zn-doped magnetic nanoparticle .....	10
7. Measurement of proliferation.....	11
8. Reverse transcription-polymerase chain reaction .....	12
9. Fate confirmation of Zn-doped magnetic nanoparticle-neural stem cells by immunocytochemistry .....	12
10. $\beta$ -catenin nuclear trans-location .....	13
11. Reporter assay .....	13

12. Western blotting -----	13
13. Quantitative real-time reverse transcription-polymerase chain reaction ---	14
14. Immunohistochemistry -----	17
15. Middle cerebral artery occlusion animal model -----	18
16. Blood brain barrier disruption -----	18
17. Intra-arterial cell injection -----	18
18. Magnetic resonance imaging -----	20
19. Bioluminescence imaging -----	20
20. Assymetric cylinder neurological test -----	22
21. Statistical analysis -----	22
22. Code of ethics and law -----	22
III. RESULTS -----	23
1. Human neural stem cell form self-renewing neurospheres and have multipotency -----	23
2. Firefly luciferase expressing neural stem cells -----	23
3. Zn-doped magnetic nanoparticle properties and intracellular labeling ----	25
4. Magnetotactic ability of Zn-doped magnetic nanoparticle neural stem cells -----	27
5. Effects if Zn-doped magnetic nanoparticle in neural stem cell homeostasis -----	30
6. Neuronal differentiation of Zn-doped magnetic nanoparticle-neural stem cells -----	33

7. Blood brain barrier disruption -----	44
8. Tracking cell migration path -----	44
9. Measuring engrafted cell number -----	50
10. Therapeutic effect -----	50
IV. DISCUSSION -----	56
V. CONCLUSION -----	60
REFERENCES -----	62
ABSTRACT (IN KOREAN) -----	67





## LIST OF FIGURES

Figure 1. Middle cerebral artery occlusion animal model -----	19
Figure 2. Neural stem cell characterization -----	24
Figure 3. Firefly luciferase and GFP expressing neural stem cells ---	26
Figure 4. Zn-doped magnetic nanoparticle and intracellular labeling -----	28
Figure 5. Zinc ion staining -----	29
Figure 6. <i>In vitro</i> magnetotactic migration -----	31
Figure 7. <i>In vivo</i> magnetotactic migration -----	32
Figure 8. Zn-doped magnetic nanoparticle mediated apoptosis -----	34
Figure 9. Zn-doped magnetic nanoparticle mediated genotoxicity ---	35
Figure 10. Neurosphere assay -----	36
Figure 11. BrdU proliferation assay -----	37
Figure 12. Genetic screening and differentiation patterns <i>in vitro</i> ----	39
Figure 13. Zn-doped magnetic nanoparticle mediated activation of Wnt signaling pathway -----	41
Figure 14. Western blot analysis and Quantitative polymerase chain reaction analysis -----	42

Figure 15. Mechanism of Zn-doped magnetic nanoparticle mediated neural stem cell neurogenesis -----	43
Figure 16. Increased neuronal differentiation of ZnMNP-neural stem cells <i>in vivo</i> -----	45
Figure 17. Blood brain barrier disruption in stroke -----	46
Figure 18. MRI based <i>in vivo</i> tracking of cellular path in ischemic brain-----	47
Figure 19. Histological tracking of cellular path in ischemic brain --	48
Figure 20. Engraftment of injected cells in ischemic brain -----	51
Figure 21. Therapeutic potentials of magnetically guided Zn-doped magnetic nanoparticle-neural stem cells in ischemic brain -----	53
Figure 22. Magnetic nanoparticles control neural stem cell behavior in ischemic brain -----	59

## LIST OF TABLES

Table 1. Antibodies used for immunostaining -----	7
Table 2. Sequences of primers used for polymerase chain reaction --	15
Table 3. Antibodies used for western blotting -----	16
Table 4. Sequences of primers used for Quantitative polymerase chain reaction -----	21
Table 5. Differentiation pattern of Zn-doped magnetic nanoparticle- neural stem cells <i>in vitro</i> and <i>in vivo</i> -----	40
Table 6. Differentiation pattern of Zn-doped magnetic nanoparticle- neural stem cells in stroke brain -----	49
Table 7. Engraftment of magnet guided Zn-doped magnetic nanoparticle-neural stem cells in stroke brain -----	52
Table 8. Infarction volume measurement -----	54
Table 9. Assymmetric neurological cylinder test -----	55

# Curriculum Vitae

(Updated in 2015.December)

**Seokhwan Yun**

## A. Education and Training

2007-2015      Doctoral course - Regenerative medical science  
2005-2007      Master`s course – Neuroscience  
2010-2012      Technical Research Personnel

## B. Journal Publish

**1. 2008. Thesis of Master`s Degree.** Yonsei University College of Medicine  
Manufacture of GDNF (Glial cell line-derived neurotrophic factor) or VEGF (Vascular endothelial growth factor) expressing recombinant adenovirus using CAG promoter and transplantation of GDNF or VEGF expressing human neural stem cells(hNSCs) into SOD1(G93A) ALS(amyotrophic lateral sclerosis) mice

Korean Library of Congress, Code number : TM 616.8    477c

**2. 2009. Journal Publish.** Experimental and Molecular medicine (EMM)  
Growth factor-expressing human neural progenitor cell grafts protect motor neurons but do not ameliorate motor performance and survival in ALS mice

DOI: 10.3858/emm.2009.41.7.054

**3. 2014. Journal Publish.** ACS nano  
T1 and T2 dual-mode MRI contrast agent for enhancing accuracy by engineered nanomaterials.

DOI: 10.1021/nn405977t

**4. 2014. Journal Publish.** Plos One

Human fetal brain-derived neural stem/progenitor cells grafted into the adult epileptic brain restrain seizures in rat model of temporal lobe of epilepsy

DOI: 10.1371/journal.pone.0104092

**5. 2014. Journal Publish.** Scientific reports

Real-time discrimination between proliferation and neuronal and astroglial differentiation of human neural stem cells

DOI: 11.1186/s13024-015-0035-6

**6. 2015. Journal Publish.** Molecular neurodegeneration

Human neural stem cells alleviate Alzheimer-like pathology in a mouse model

DOI: 10.1038/srep06319

**7. 2015. Journal Publish.** Neural plasticity

Clinical trial of human fetal brain-derived neural stem/progenitor cell transplantation in patients with traumatic cervical spinal cord injury

DOI: 10.1155/2015/630932

**8. 2015. Journal Publish.** Nature nanotechnology - in submission progress

Magnetic nanoparticles control neural stem cell behavior in ischemic injured brain

**9. 2015. Journal Publish.** ACS nano - in submission progress

SLIDING fibers: *SLID*able, *IN*jectable, and *Gel*-like electrospun nanofibrous scaffolds

**10. 2015. Thesis of Doctoral Degree.** Yonsei University College of Medicine

Magnetic nanoparticles control neural stem cell behavior in normal and ischemic brain

**C. Patent**

1. 자성나노입자를 포함하는 신경세포 분화 촉진용 조성물 (in progress)

## **D. Presentation in International Association**

- 1. 2006.** Society for Neuroscience(SFN) 36th annual meeting, Atlanta, GA, USA  
Cell and gene therapy via human neural stem cells in transgenic SOD1 (G93A) ALS (amyotrophic lateral sclerosis) mice.
- 2. 2007.** 5th ISSCR annual meeting, Queensland, Australia  
Transplantation of human neural stem cells into transgenic SOD1 (G93A) ALS (Amyotrophic lateral sclerosis) mice
- 3. 2007.** The Korean Society for neurodegenerative disease, Seoul, Korea  
Transplantation of human neural stem cells into transgenic SOD1(G93A) ALS(amyotrophic lateral sclerosis) mice
- 4. 2008.** Society for Neuroscience(SFN) 38th annual meeting, Washington DC, USA  
Transplantation of TRAIL (Tumor necrosis factor-related apoptosis-inducing ligand) and SMAC (second mitochondria-derived activator of caspase) expressing human neural stem cells (hNSCs) synergistically induces apoptosis of intracranial glioblastoma
- 5. 2008.** Seoul Symposium on Stem cell research, Yonsei university, Seoul, Korea  
Neurotrophic factor expressing human neural progenitor cell grafts protect motor neurons, but do not ameliorate motor performance and survival in SOD1 transgenic mice,
- 6. 2008.** Society for Neuroscience(SFN) 38th annual meeting, Washington DC, USA  
Neurotrophic factors expressing human neural progenitor cells grafts protect motor neurons, but do not ameliorate motor performance and survival in SOD1 transgenic mice
- 7. 2009.** National Core Research Center, Wonju, Korea  
Nanoparticle mediated human neural stem cells(hNSCs) migration
- 8. 2010.** 2nd World Congress on Tissue engineering & Regenerative Medicine  
International Society (TERMIS), Galway, Ireland  
Growth factor-expressing human neural progenitor cell grafts protect motor neurons but do not ameliorate motor performance and survival in ALS mice.
- 9. 2010.** 8th Annual meeting of ISSCR, San Francisco, CA, USA  
Transplantation of human neural stem cells suppresses seizure activity in rat model of temporal lobe epilepsy.
- 10. 2010.** Society for Neuroscience(SFN) 40th annual meeting, Chicago, USA  
Transplantation of human neural stem cells suppresses seizure activity in rat model of temporal lobe epilepsy.

- 11. 2010.** Society for Neuroscience(SFN) 40th annual meeting, Chicago, USA  
Transplantation of human neural stem cells-derived oligodendrocyte precursor cells into contusive spinal cord injury in adult rats.
- 12. 2010.** 8th Seoul Symposium on Stem Cell Research. Yonsei university, Seoul, Korea  
Transplantation of human neural stem cells suppresses seizure activity in rat model of temporal lobe epilepsy.
- 13. 2010.** National Core Research Center, Wonju, Korea  
Nanoparticle mediated human neural stem cells(hNSCs) differentiation
- 14. 2011.** Seoul Symposium on Stem Cell Research, Yonsei university, Seoul, Korea  
Transplantation of human neural stem cells-derived oligodendrocyte precursor cells which obtained from different fetal brain regions at diverse gestational ages into contusive spinal cord injury in adult rats
- 15. 2011.** Society for Neuroscience(SFN) 40th annual meeting, Washington DC, USA  
Transplantation of human neural stem cells-derived oligodendrocyte precursor cells which obtained from different fetal brain regions at diverse gestational ages into contusive spinal cord injury in adult rats.
- 16. 2014.** Society for Neuroscience(SFN) 44th annual meeting, Washington DC, USA  
Human fetal brain-derived neural stem/progenitor cells grafted into the adult epileptic brain restrain seizures in rat models of temporal lobe epilepsy.
- 17. 2015.** 13th Annual meeeting of ISSCR, San Francisco, Stockholm, Sweden  
Human neural stem cell transplantation ameliorate Alzheimer's disease-like pathology in a mouse model via multiple mechanisms.
- 18. 2015.** Korean Society for Stem cell research, Seoul, Korea  
Human neural stem cell transplantation ameliorate Alzheimer's disease-like pathology in a mouse model via multiple mechanisms.

ABSTRACT

**Magnetic nanoparticles control neural stem cell behavior  
in normal and ischemic brain**

Seokhwan Yun

*Department of Medical Science*

*The Graduate School, Yonsei University*

(Directed by Professor Kook In Park)

Over the past few decades, the establishment of neural stem cells as a long-lasting source of neurons and glial cells had led to the development of novel therapeutic approaches for a variety of neurodegenerative disorders such as brain stroke. Neural stem cells graft promoted brain protection, regeneration and functional recovery. Nonetheless, the therapeutic benefits of neural stem cells had been limited due to their poor *in vivo* control of migration, engraftment and differentiation into target tissue.

Recently, nanotechnologies are emerging platforms that could be useful in measuring, understanding and manipulating stem cells. Advanced nanoparticles, carbon nanotubes, and polyplexes have been widely used for stem cell labeling, tracking, differentiation and transplantation.

Here we demonstrated magnetotactic human neural stem cells that can be directed to the desired target lesion *via* non-invasive, remote magnetic guidance. In the presence of an external magnetic field, the advanced magnetic nanoparticle allowed neural stem cells to possess strong attraction forces, which was sufficient for migration, and highly sensitive MRI contrast that enabled long-term tracking of neural stem cells. We found the enhanced migration and engraftment and promoted neuronal differentiation of non-invasively injected magnetotactic neural stem cells in animal stroke model which resulted in improved neurological function and pathology.



**Key words** : magnetic nanoparticles, neural stem cells, stroke, cell therapy, magnetotaxis

**Mangetic nanoparticles control neural stem cell behavior  
in normal and ischemic brain**

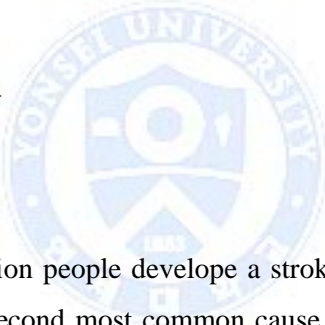
Seokhwan Yun

*Department of Medical Science*

*The Graduate School, Yonsei University*

(Directed by Professor Kook In Park)

**I. INTRODUCTION**



Worldwide, around 15 million people develop a stroke every year and with about 5 million deaths, stroke is the second most common cause of death and a major cause of long-term disability.<sup>1,2</sup> It is estimated that about 25% of people older than 85 years will develop stroke. In the past decade, remarkable progress in understanding stroke pathophysiology has been made, especially in ischemic stroke,<sup>1,3</sup> which makes up 80% of all cases.<sup>3</sup> These advances have led to the identification of more than 1,000 molecules with brain-protective effects from experimental models and to the implementation of more than 250 clinical trials.<sup>4</sup> Despite all these efforts, there have been no effective treatment. Current therapeutic approaches, such as the use of thrombolytics, benefit only 1% to 4% of patients.<sup>4</sup> Recent evidence suggested that the transplantation of stem cells derived from cord blood or bone marrow or brain-derived neural stem cell resulted in functional recovery in experimental models of stroke.<sup>1-3</sup>

Like other stem cells, neural stem cells (NSCs) possess the unique property of self-renewal and the ability to generate differentiated progeny that can be utilized to generate

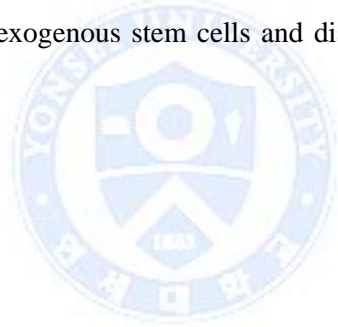
both neurons and glial cells.<sup>5-7</sup> Thus, NSCs transplanted to neuronal injury or degeneration in the central nervous system (CNS) can not only promote the replacement of damaged tissue, but also support neuroprotection by preventing tissue injury and rescuing host cells.<sup>8,9</sup> Because of harsh biological environments in areas of pathology, NSCs were usually transplanted somewhat distant from target lesions to secure cellular viability and engraftment. Owing to the chemotactic nature of NSCs, they could migrate towards diseased areas in response to a chemical gradient induced by lesions.<sup>10,11</sup> Because the therapeutic effects of NSCs vary depending on homing efficiency to areas of pathology, efficient migration with high engraftment and viability is regarded as one of the critical requirements for successful stem cell therapy.<sup>4,8</sup> However, delivery of stem cells through chemotaxis was often limited by low homing efficiency due to complicated chemo-attractive mechanisms that hinder accurate manipulation and/or guidance of stem cells. Several attempts to overcome such obstacles have been made using a direct intracerebral transplantation strategy, which allows for increased efficiency of NSC homing.<sup>10,12,13</sup> However, this strategy is used reluctantly because of its associated invasiveness, which includes craniectomy.

The term, magnetotaxis, is a composite word of magnet and chemotaxis. Magnetotaxis were chosen as an alternative solution of chemotaxis owing to the development of magnetic nanoparticle. Zinc-doped iron oxide magnetic nanoparticles ( $Zn_{0.4}Fe_{2.6}O_4$ , ZnMNP, 18 nm diameter) have superparamagnetic properties and higher saturation magnetization (Ms) value (161 emu/g) than Ms value of ferumoxide (78emu/g) that have been approved by the U. S Food and Drug Administration (FDA).<sup>14</sup> ZnMNP gave rise to cells not only magnetotactic ability but also provided several biomedical advantages such as Magnetic Resonance imaging (MRI) tracking, drug delivery and hyperthermia.<sup>15</sup>

To attempt cell based therapy, tracking cellular path in animal model is crucial.<sup>16</sup> Various histological methods provide high resolution of exogenous cell image, but those methods could provide information only at the time of sacrificing animal. An important goal in stem cell therapy is observation of donor-derived cells *in vivo* to survey their engraftment, location. MRI is one of the powerful tools that is suitable for this purpose.

Researchers have tried to use MRI to track transplanted cells.<sup>17,18</sup> Superparamagnetic iron oxide (SPIO) nanoparticles produce hypo-intense dark signal in T2-weighted image.<sup>17,18</sup> However, visualization cells by MRI *in vivo* have limits such as false signal by artifact, low resolution compared to histologic images. Such obstacles can be overcome by ZnMNP due to the strong Ms value.

Taken advantages of both ZnMNP and NSCs, we transfected ZnMNP to NSCs, and intravascular cell injection into middle cerebral artery occlusion (MCAO) animal model penetrated the damaged brain through disrupted blood brain barrier (BBB), engraftment and migration to ischemic core and penumbra area by static magnetic field. In addition, exogenous cells were capable of tracing non-invasively with MRI and bioluminescence imaging (BLI). Furthermore, ZnMNP transfection cause neuronal differentiation of NSCs through wnt/ $\beta$ -catenin signaling pathway. Combination of these properties, we anticipated to regulate, trace exogenous stem cells and discover a new therapeutic stem cell application method.



## **II. MATERIALS AND METHODS**

### **1. Culture of human neural stem cells**

Human fetal tissue aborted at 13 weeks of gestation was provided with full patient consent and the approval of the research ethics committee of Yonsei University College of Medicine.<sup>19</sup> The method of acquisition confirmed to National Institutes of Health (NIH) and Korean Government guidelines. Human NSCs were isolated from fetal telencephalic brain tissue by chopping and trypsinization and seeded into tissue culture-treated 100 mm plates (Corning, Lowell, MA, USA) at a density of 200,000 cells/ml of serum-free growth medium and Ham's F12 (DMEM/F12; Gibco, Carlsbad, CA, USA) supplemented with N2 formulation (Gibco). Mitogenic stimulation was achieved by adding 20 ng/ml fibroblast growth factor (FGF2; R&D Systems, Minneapolis, MN, USA) and 10 ng/ml leukemia inhibitory factor (LIF; Sigma, St. Louis, MO, USA). Heparin (8 µg/ml; Sigma) was added to stabilize FGF-2 activity.<sup>19</sup> All of the cultures were maintained in a humidified incubator at 37°C and 5% CO<sub>2</sub> in air, and half of the medium was replenished every 3-4 days. Passaging was undertaken every 7-8 days by dissociation of bulk neurospheres with 0.05% trypsin/EDTA (T/E; Gibco).<sup>19</sup> The neurospheres were re-seeded into fresh growth medium at a density equivalent to approximately 200,000 cells/ml. Some neurospheres were attached on silane coating slide glass (Mutoglass, Japan) by use of cytospin (Shandon, Albany, NY, USA) for NSC characterization. 2 µM 5-bromo-2'-deoxyuridine (BrdU) was added to cultures 48 hours prior to cytospin attachment. Attached neurospheres were immunostained with proliferating markers, neural stem cell markers and several neurotrophic factors (Table. 1). In differentiated conditions, trypsinized single cells were re-seeded in PLL coated 8-well chamber slide (Corning, Lowell, MA, USA) and immunostained with lineage specific antibodies (Table. 1).

## **2. Firefly luciferase expressing neural stem cells**

Recombinant lenti-viruses were produced using transient transfection into 293FT cells. Subconfluent 293FT cells were cotransfected with 20 µg pWPI transfer plasmid vector containing firefly luciferase (Fluc) with Green Fluorescent Protein (GFP), 15 µg psPAX2 packaging construct plasmid and 6 µg pMD2G envelop plasmid by calcium phosphate precipitation. The lentiviral plasmid vectors were donated from Trono lab (<http://tronolab.epfl.ch>). After 3 hours, the media was changed with fresh medium, recombinant viruses were harvested 48 hours later and viruses were concentrated by ultracentrifugation under the sucrose cushion buffer. The virus titer was checked as transducing unit (TU) via flow cytometry (Vector Dickson, Dickson city, PA, USA).<sup>20</sup> To transduce recombinant lenti-viruses, NSCs were seeded onto cell culture dishes (Corning). 1 hour later, lentiviral particles were added to well. The media was replaced with fresh one the next day, and each cells transduced with lentiviral vector were cultured over 1 month to confirm the stable expression of Fluc and GFP.

## **3. Synthesis of Zn-doped magnetic nanoparticle**

Zinc doped iron oxide magnetic nanoparticles ( $Zn_{0.4}Fe_{2.6}O_4$ , ZnMNPs) were prepared by thermal decomposition of  $Fe(acac)_3$  (Sigma, 353 mg),  $ZnCl_2$  (Sigma, 30 mg) and  $FeCl_2$  (Sigma, 40 mg) in octyl ether containing oleic acid and oleylamine. The mixture was heated at 300°C for 1 hour. After removing the heat source, the reaction products were cooled to room temperature. The color of reaction mixture turned black and we obtained 18 nm ZnMNPs. Upon addition of ethanol, a black powder was precipitated and isolated by centrifugation. The isolated ZnMNPs were dispersed in a solvent such as toluene. The organic surfactants on the ZnMNPs surface were removed and exchanged with dextran to

make the ZnMNPs dispersed in the aqueous medium completely.<sup>14</sup>

**Table 1. Antibodies used for immunostaining**

<b>Antibodies<sup>1</sup></b>	<b>Host</b>	<b>Titer</b>	<b>Company</b>	<b>Domicilli</b>
<b>β-catenin</b>	rabbit	1:200	Cell signaling	Danvers, MA, USA
<b>BDNF</b>	rabbit	1:1000	Santacruz	Dallas, CA, USA
<b>BrdU-FITC</b>	mouse	1:20	Roche	Penzberg, German
<b>Caspase3</b>	rabbit	1:250	BD	Franklin Lakes, NJ, USA
<b>CD133</b>	goat	1:100		
<b>Dcx</b>	goat	1:400		
<b>FGF</b>	rabbit	1:1000	Santacruz	Dallas, CA, USA
<b>GDNF</b>	rabbit	1:1000		
<b>GFAP</b>	rabbit	1:1500	DAKO	Glustrup, Denmark
<b>GFP</b>	rabbit	1:200	Invitrogen	Waltham, MA, USA
<b>hNuc</b>	mouse	1:100	Chemicon	Darmstadt, German
<b>KI67</b>	mouse	1:100	DAKO	Glustrup, Denmark
<b>Map2</b>	rabbit	1:500	Cell signaling	Danvers, MA, USA
<b>Nestin</b>	rabbit	1:200		
<b>Nestin</b>	mouse	1:200	Chemicon	Darmstadt, German
<b>NGF</b>	rabbit	1:1000	Cell signaling	Danvers, MA, USA
<b>NTF3</b>	rabbit	1:1000		
<b>NTF4</b>	rabbit	1:1000	Santacruz	Dallas, CA, USA
<b>O4</b>	mouse	1:100		
<b>Olig2</b>	rabbit	1:500	Chemicon	Darmstadt, German
<b>Pax6</b>	mouse	1:100	DSHB	Iowa city, IA, USA
<b>PCNA</b>	rabbit	1:100		
<b>PDGFR</b>	rabbit	1:100	Santacruz	Dallas, CA, USA
<b>Sc121</b>	mouse	1:500	SC-proven	Newark, CA, USA
<b>Sox2</b>	rabbit	1:200	Chemicon	Darmstadt, German
<b>Tuj1</b>	rabbit	1:500	Covance	Princeton, NJ, USA
<b>VEGF</b>	rabbit	1:1000	Santacruz	Dallas, CA, USA
<b>Vimentin</b>	mouse	1:40	Sigma	St. Louis, MO, USA

<sup>1</sup> Antibodies were listed in alphabetical order.

#### **4. Intracellular labeling of Zn-doped magnetic nanoparticle to neural stem cells**

For the intracellular labeling of NSCs with ZnMNP, trypsinized single NSCs (or Lenti-Fluc-GFP-NSCs) were plated with half volume of growth medium at a final cell density of  $3 \times 10^6$  cells/well in 6well culture plate (Corning). ZnMNP solutions were prepared at a 2× concentration in growth medium then poly-L-lysine (PLL; Sigma) from stock solution (1 mg/ml) was added and allowed 5 minutes at RT. 1ml of 2× ZnMNP-PLL solutions were added to 1ml of NSCs suspensions (final concentration of ZnMNP-PLL was 15µg/ml in growth medium) and incubated for 48 hours. Cells in growth medium without ZnMNP were used as an untreated control. 48 hours later, cells were refreshed with new growth medium and incubated for 24 hours more. At the end of the incubation, cells were treated with 0.05% T/E (Gibco), triturated mechanically, washed three times with Hank's-HEPES buffer solution (1× Hanks' balanced salt solution, 10mM HEPES, pH 7.4; Gibco).

For Perl's prussian blue staining, which indicates the presence of iron, cells were treated with 0.05% T/E (Gibco) and resuspended in N2 media ( $4 \times 10^4$  cells/200µl). Subsequently, cells were attached on silane coating slide glass (Mutoglass, Japan) by use of cytopsin (Shandon). Cells were fixed with 95% EtOH, washed, incubated for 10 minutes with 5% potassium ferrocyanide in 1N hydrochloric acid, washed again, and counterstained with nuclear fast red for 1 minute.<sup>21</sup> Images were obtained using fluorescence microscopy (Olympus, Tokyo, Japan)

Internalization of the nanoparticle was visualized with electron microscopy using standard protocols.<sup>22</sup> Cells were trypsinized and fixed with 2% glutaraldehyde + 2% paraformaldehyde in 0.1 M phosphate buffered saline at 4°C, 24hours. Sampling was processed with standard electron microscopy procedures and examined with a JEOL JEM-1011 transmission electron microscope (Jeol, Japan).

Zn ion level was measured by use of FluoZin<sup>TM</sup>-3, AM (Invitrogen, Waltham, MA, USA). FluoZin<sup>TM</sup>-3, AM dissolved in DMSO (Sigma), were mixed with 1:1 with Pluronic acid (Sigma, 20% in DMSO) to improve dispersion in the aqueous media.<sup>23-25</sup> Mixture of Zn ion indicators were added to cell culture media 1 hour and were fixed by 4% PFA. Images were obtained using fluorescence microscopy (Olympus) and fluorescence level was measured by flow cytometry (Dickson). For positive control groups, NSCs were treated to 0.5 $\mu$ M ZnCl<sub>2</sub> 1 hour.

## 5. Magnet guided cell delivery *in vitro* and *in vivo*

0.2% agarose gel (weight/volume) was used to develop a robust model of intraparenchymal brain tissue for the purpose of simulating cell migration in brain tissue.<sup>26,27</sup> This brain mimicking *in vitro* model consisted of two different compartments; one was agarose gel which is known to similar density with brain tissue, the other was capillary tube containing phosphate buffered saline (PBS) which mimics the blood vessel environment. For visualization of the cell migration, we used Lenti-Fluc-GFP-NSCs. 3 group of cells (ZnMNP-Lenti-Fluc-GFP-NSCs, FeMNP-Lenti-Fluc-GFP-NSCs and Lenti-Fluc-GFP-NSCs) were loaded to the capillary tube and exposed to the magnetic field. After applying magnetic field for 12 hours, luciferase activity was visualized every 2-3 hours.

*In vivo* magnetic cell guidance experiment was performed using adult male Sprague-Dawley (SD) rats weighing 250 $\pm$ 10g. This animal experiment was performed in strict accordance with the recommendation in the Guide for the Care and Use of Laboratory Animals of the National Institute of Health. Also the protocol was approved by the committee in the Ethics of Animal experiments of Yonsei University College of Medicine (Permission number, 2013-0135). All animals were purchased from the same commercial breeder (Orient, Korea) and were housed in the same specific pathogen free (SPF) facility under a 12 hours light/dark cycle with ad libitum feeding. Lenti-Fluc-GFP-ZnMNP-NSCs



were transplanted into the rat brains. Animals were anaesthetized with 2.5% isoflurane (Hanapharma, Busan, Korea) with oxygen and the skull was exposed. Total number of  $1.2 \times 10^5$  cells in  $4 \mu\text{l}$  was transplanted using a hamilton syringe (Hamilton Com., NV, USA), into the right corpus callosum at the following stereotaxic coordinates in millimeters (AP 0 mm, ML 0.5 mm, and DV 4.0 mm from the bregma). Unlike other usual experiment using stereotaxic frame, we did not use vertical injection to avoid the rough leaking of transplanted cells. Instead, injections needles entered obliquely at 45 degree by use of trigonometrical calculation. The injection rate was  $1 \mu\text{l}/\text{min}$  and the hamilton syringe was left in place for 5 minutes before retraction. 24 hours after transplantation, neodymium (10mm diameter) was implanted above the skull bregma.

## 6. Cytotoxicity of Zn-doped magnetic nanoparticle

Cell viability was assessed using Cell Counting kit-8 (CCK8; Dojingo Molecular Technologies, Inc, Rockville, MD, USA) containing WST-8 (2-(2-methoxy-4-nitrophenyl)-3-(4-nitrophenyl)-5-(2,4-disulfophenyl)-2H-tetrazolium, monosodium salt), which is reduced by dehydrogenases in cells to give a yellow-colored product, formazan. The amount of the formazan dye generated by the activity of dehydrogenases in cells is directly proportional to the number of living cells, thus allowing estimation of the number of viable cells in the medium by absorbance at 450nm.

Cytotoxicity was assessed immunostaining of active caspase-3<sup>28</sup> and transferase dUTP nick and labeling (TUNEL) staining<sup>29</sup> *in vitro* to confirm cytotoxicity at 3 days after transfection. Cells were treated with 0.05% T/E (Gibco) and resuspended in N2 media. Subsequently, cells were attached on saline coating slide glass (Mutoglass) by use of cytospin (Shandon) and performed immunocytochemistry with the rabbit anti-caspase 3 antibody (Table. 1). The secondary antibody used were FITC-conjugated anti-rabbit-IgG. TUNEL assay was performed using In Situ Cell Detection kit (Roche Applied Science, Indianapolis, IN, USA). Cells were fixed with 4% paraformaldehyde (PFA) in PBS for 1

hour at room temperature. The samples were washed with PBS and then permeabilized by 0.1% Triton X-100 in 0.1% sodium citrate buffer for 15 minutes at 4°C. After 3 times washing, cells were treated with TUNEL reaction mixture (Roche Applied Science) and incubated for 60 minutes at 37°C. Images were obtained using fluorescence microscopy (Olympus).

Reactive oxygen species (ROS) was measured using 6-carboxy-2',7'-dichlorodihydrofluorescein diacetate (DCFH-DA, Sigma).<sup>30</sup> Briefly, cells were seeded onto 96-well black plates at a density of 5,000 cells/well. 24 hours after seeding, cells were washed with PBS, treated with 100µM DCFH-DA in cell culture media for 1 hour. Cells were then washed with PBS again and lysate with Tissue Protein Extraction Reagent (T-PER; Thermo Fisher Scientific). ROS level was measured by luminescence spectrometer LS50B (Perkin Elmer Akron, OH, USA) and normalized to protein concentrations, For positive control groups, NSCs were exposed to ultraviolet (UV) 20 minutes.

Next, we measured DNA damage by use of comet assay, based on gel electrophoresis method.<sup>31</sup> Slide glass were coated with mixture of low melting agarose solution (Sigma) and trypsinized cell. Coated slide glasses were treated by 0.5M Na<sub>2</sub>EDTA (pH8.0) solution for 24 hours at 4°C, and conducted electrophoresis for 25 minutes at a voltage of 0.6V/cm. Subsequently, slide samples were treated with Dapi (Vector). Images were obtained using fluorescence microscopy (Olympus).

## **7. Measurement of proliferation**

NSCs proliferation was determined by quantifying DNA replication using Bromodeoxyuridine (5-bromo-2'-deoxyuridine, referred to BrdU), a thymidine analogue, which enables the detection of actively proliferating cells that have progressed in S phase.<sup>32</sup> Cells were seeded onto 6 well culture dishes at approximately 1X10<sup>6</sup> cells/well

without mitogen for 24 hours to stop the cell cycles. Cells were next incubated with BrdU at a final concentration of 2 $\mu$ M for 3 days and were fixed with a 100% ethanol. After cell membrane permeabilization using 2N hydrochloric acid (HCl), the cells were labeled with a fluorescein (FITC) conjugated anti-BrdU antibody (Sigma). Cells were counted by flow cytometry (Dickson).

## **8. Reverse transcription-polymerase chain reaction**

Total Ribonucleic acid (RNA) was prepared from cell using TRI Reagent® (Molecular Research Center, Inc, Cincinnati, OH, USA). RNAs were quantified spectrophotometrically, and then 5 $\mu$ g of isolated RNA was reverse transcribed using Superscript<sup>TM</sup>III Reverse Transcriptase (Invitrogen) in 20 $\mu$ l reaction volume for complementary deoxyribonucleic acid (cDNA) synthesis. Therefore, 1 $\mu$ l cDNA was used for polymerase chain reaction (PCR) in 20 $\mu$ l volume. Primer pairs were designed and customized to detect target gene (Table. 2). PCR products were confirmed with 1.5% agarose gel electrophoresis and staining of ethidium bromide (EtBr, Sigma).

## **9. Fate confirmation of Zn-doped magnetic nanoparticle-neural stem cells by immunocytochemistry**

Trypsinized NSCs were dissociated into a single cell suspension and directly plated onto PLL (10 $\mu$ g/ml, Sigma) in DMEM/F-12 that contained N2 supplement without any mitogens. The cells were fixed on 7 days with 4% PFA for 20 minutes, rinsed three times with PBS, and immunostained with lineage specific antibodies (Table. 1 ; Nestin, GFAP, Tuj1).<sup>19</sup> Following rinsing with PBS, the slides were incubated with species specific secondary antibodies conjugated with FITC or Texas Red (Vector). Dapi was

used as the nuclear staining. Images were obtained using fluorescence microscopy (Olympus).

#### **10. $\beta$ -catenin nuclear trans-location**

To evaluate the level of  $\beta$ -catenin expressed in the cell nucleus, we plated trypsinized single cells on PLL-coated 8 well chamber slides and immunostained with antibody against  $\beta$ -catenin (Table. 1). Images were obtained using fluorescence microscopy (Olympus). We quantified the intensities of the pixels in each channel (Dapi; blue,  $\beta$ -catenin; green) in the sections and generated histogram by use of photoshop CS3 software (Adobe systems, San Jose, CA, USA). The levels of  $\beta$ -catenin were determined and mean values calculated within the cell nucleus (Dapi).<sup>33</sup>



#### **11. Reporter assay**

Cells were transfected with reporter plasmids (TCF/LEF promoter following Firefly luciferase containing plasmid and CMV promoter following Renilla luciferase containing plasmid; 40:1) by Attractene Transfection Reagent 301004 (Qiagen, Valencia, CA, USA).

We measured luciferase activity 120 hours after transfection in 50 $\mu$ l of lysis supernatant with the Cignal Reporter Assay system (Qiagen). The Firefly luminescence signal was quantified with a luminometer (Berthold, Wilbad, Germany) and normalized by Renilla luminescence signal.<sup>34</sup> This analysis was conducted not just neural stem cells, but MDA-MB-231 cells (breast cancer cell line) and HEK 293 cells (human embryonic kidney cell line).

#### **12. Western Blot analysis**

Protein samples were prepared in two different types; cell lysate and cell culture conditioned medium. Cell lysate samples were prepared using homogenization in Tissue Protein Extraction Reagent (T-PER; Thermo Fisher Scientific, Suwanee, GA) supplemented with protease inhibitors (Sigma). Cell culture conditioned medium was concentrated 10-fold using Amicon Ultra-0.5 centrifugal filter device (Millipore, Darmstadt, German). Both protein samples were resolved by sodium dodecyl sulfate-polyacrylamide gel electrophoresis (SDS-PAGE). Samples were loaded onto 10% tris-glycine gels, and the proteins were transferred from the gel onto a 0.45 $\mu$ m nitrocellulose membrane (Thermo Scientific) over 4 hours at 4 $^{\circ}$ C. The protein blots were blocked with 5% skimmed milk in TBST and incubated with 0.25 bovine serum albumin in tris-buffered saline and tween 20 (TBST) overnight at 4 $^{\circ}$ C with the primary antibodies (Table. 3). Then, protein included membranes were rinsed with TBST, incubated with a horseradish peroxidase-conjugated secondary antibodies, for 1 hour at room temperature, and developed using SuperSignal West Pico Chemiluminescent substrate (Thermo Scientific).<sup>35</sup> The images were scanned with a Fujifilm LAS-4000 mini-imager and band densities were measured by ImageJ software (<http://imagej.nih.gov/ij/>). In cell lysate samples, band densities were normalized by the density of  $\beta$ -actin. In cell culture medium samples, band densities were normalized by the density of the 75 kDa ponceau red staining band.

### **13. Quantitative real-time reverse transcription-polymerase chain reaction**

Total RNA was prepared from cell using TRI Reagent (Molecular Research Center), and 2 $\mu$ g of RNA was reverse-transcribed into cDNA using random hexamer primers (Bioneer, Daejeon, Korea) and Superscript III reverse transcriptase (Invitrogen) in a thermal cycler (Eppendorf, Happauge, NY, USA). Quantitative RT-PCR was carried out in a total volume of 10 $\mu$ l containing 5 $\mu$ l of LightCycler<sup>®</sup> 480SYBRGreen I Master (Roche

Diagnostics Ltd., Rotkreuz, Switzerland), 0.5µM of each primer and 2.5µl of 1:10 diluted cDNA using LightCycler® 480 instrument (Roche Diagnostics Ltd). The cycling conditions

**Table 2. Sequences of primers used for RT-PCR**

<b>Gene</b>	<b>Gene Bank ID<sup>1</sup></b>	<b>Primers (5'→3')<sup>2</sup></b>
<i>Wnt1</i>	NM_005430.3	5'-CGGCGTTTATCTTCGCTATCA-3' 5'-GCAGGATTTCGATGGAACCTTCT-3'
<i>Wnt3a</i>	NM_033131	5'-AGTACCCGATCTGGTGGTC-3' 5'-CAAACCTCGATGTCCTCGCTAC-3'
<i>Nestin</i>	NM_006617	5'-TGGAGTCTGTGGAAGTGAACC-3' 5'-CATTTTCCACTCCAGCCATCC-3'
<i>Sox2</i>	NM_181701	5'-CTCGTGCAGTTCTACTCGTCG-3' 5'-AGCTCTCGGTCAGGTCCTTT-3'
<i>Neurog2</i>	NM_024091	5'-CGAAACCGCATGCACAACCTC-3' 5'-TGGAATTGGAGGACACGGAGG-3'
<i>NeuroD1</i>	NM_002500	5'-GCTGCCAGTCCGCCTTACG-3' 5'-CTCGGCGGACGGTTCGTGTT-3'
<i>ASCL1</i>	NM_034316	5'-GGCTCAACTTCAGCGGCTT-3' 5'-CAGTGTCTCCACCTTACTCATCT-3'
<i>Tuj1</i>	NM_006086	5'-CCGAGCTCACCCAGCAGATGT-3' 5'-AACATGGCCGTGAACTGCTCG-3'
<i>SGC10</i>	S82024.1	5'-CATCAACATCTATACTTACG-3' 5'-GCCAATTGTTTCAGCACCTG-3'
<i>Tbr2</i>	AB_031038.1	5'-ACATTGCTCCCATATGGCATT-3' 5'-CCTTCGCTTACAAGCACTGGT-3'
<i>GAD65</i>	NM_001134366	5'-TTTTGGTCTTTCGGGTCGGAA-3' 5'-TTCTCGGCGTCTCCGTAGAG-3'
<i>s100b</i>	NM_006272	5'-GGTGGCCCTCATCGACGTTTT-3' 5'-TCGCCGTCTCCATCATTGTCC-3'
<i>BLBP</i>	NM_001446.3	5'-TACATGAAGGCTCTAGGCGTG-3' 5'-CCACATCACCAAAAGTAAGGG-3'
<i>GS</i>	NM_001033056.3	5'-GAGGCACACCTGTAAACGGA-3' 5'-ATAGGCTCTGTCTGCTCCCA-3'
<i>NG2</i>	NM_012283	5'-ACTTTGCCACTGAGCCTTACA-3' 5'-GTTTTTCGGAGGTAGAAGAGCAG-3'
<i>Olig2</i>	NM_005806	5'-AGGACAAGAAGCAAATGACAGAG-3' 5'-AGTTGGTGAGCATGAGGATGTAGT-3'
<i>GAPDH</i>	NM_001256799	5'-ACCACAGTCCATGCCATCAC-3' 5'-TCCACCACCCTGTTGCTGTA-3'

<sup>1</sup> Query Genetic code of NCBI database (www.ncbi.nlm.nih.gov/pubmed)

<sup>2</sup> Primer sequences were obtained from the NCBI database and customized by Bioneer (Daejeon, Korea).

**Table 3. Antibodies used for western blotting**

Antibodies	Host	Size <sup>1</sup>	Titer	Company	Domicilli
<b>Wnt1</b>	rabbit	41	1:1000	Santacruz	Dallas, TX, USA
<b>Wnt3a</b>	Rat	40	1:1000	R&D	Mineapolis, MN, USA
<b>NTF3</b>	rabbit	35	1:1000	Santacruz	Dallas, TX, USA
<b>NTF4</b>	rabbit	14	1:1000		
<b>NGF</b>	rabbit	13	1:1000	Cell signaling	Danvers, MA, USA
<b><math>\beta</math>-catenin</b>	rabbit	92	1:1000		
<b>Map2</b>	rabbit	250	1:1000		
<b>Tuj1</b>	mouse	50	1:5000	Covance	Princeton, NJ, USA
<b><math>\beta</math>-actin</b>	mouse	42	1:1000	Sigma	St.Louis, MO, USA

<sup>1</sup> Size of the target protein. Unit is kDa.

were: 95°C for 5 minutes, followed by 45 cycles of 95°C for 10 seconds, and 72°C for 10 seconds. All the samples were carried out in triplicates. The expression level of each mRNA expression were normalized to the housekeeping gene GAPDH using LightCycler® 480 software, Version 1.5 (Roche Diagnostics Ltd).<sup>36</sup> Primer sequences for target genes were listed in Table. 4.

#### **14. Immunohistochemistry**

Animals were deeply anesthetized with ketamine (75mg/kg, i.p.) and xylazine (30mg/kg, i.p.) and were transcardially perfused with cold PBS followed by cold 4% PFA. Brains were then removed, post fixed, transferred in 30% sucrose in PBS for cryoprotection and frozen in O.C.T compound (Sakura Finetek, Torrance, CA, USA). Frozen samples were coronally sliced into 30 µm sections using a cryostat.

For fluorescence immunohistochemistry, sections were washed in PBS and blocked with 3% bovine serum albumin (Sigma), 10% normal horse serum (Sigma), and 0.3% Triton X-100 (Sigma) in PBS. Sections were incubated with following primary antibodies; anti-human nucleus with anti-nestin or anti-neuronal class β-tubulin III (Tuj1) or anti-Map2 or anti-DCX or anti-GFAP or anti-PDGFα (Table. 1). Images were obtained using Zeiss LSM 700 confocal microscope (Carl Zeiss, Oberkochen, Germany).

For immunoperoxidase staining, section were incubated with 0.3% H<sub>2</sub>O<sub>2</sub> in methanol for blocking endogenous peroxidase activity. Sections were incubated with anti-human specific cytoplasm SC121 (Table. 1), and were developed with diaminobenzidine (DAB; Sigma) substrate using VECORSTAIN Elite ABC kit (Vector laboratories). After the DAB reaction, samples were additionally stained for Perl's prussian blue staining and nuclear fast red.



## **15. Middle Cerebral Artery Occlusion animal model**

Adult male Sprague-Dawley (SD) rats weighing  $250\pm 10$ g were used. Ethical guidelines, purchasing and housing were the same as above method (5. Magnetic guided cell delivery). During the whole procedure, each animal was anaesthetized with 2.5% isoflurane (Hana pharm, Busan, Korea) with oxygen and body temperature was maintained  $37.0\pm 0.5^{\circ}\text{C}$  with a warm pad. Through a midline neck incision, right carotid bifurcation of rat was exposed within the carotid muscular triagle.<sup>37-40</sup> Through a right carotid bifurcation, a sterile 3-0 nylon suture (AILEE Co, Busan, Korea) was introduced into the right internal carotid artery at a distance of  $20.0\pm 0.5$ mm from the carotid bifurcation to occlude the origin of middle cerebral artery.<sup>37-41</sup> After a lapse of 30 minutes, intraluminal nylon filament was carefully removed and incision was sutured. Immediately after occlusion, neodymium magnet (10mm diameter) was implanted above the skull bregma. Surgical procedure is summarized in Figure 1.

## **16. Blood Brain Barrier Disruption**

BBB disruption was examined by injecting evans blue (Sigma) to femoral vein (0.05% Evans blue in PBS, 1ml/kg) of MCAO animal.<sup>40</sup> After a lapse of 4 hours, transcardiac perfusion with PBS slowly and brain was dissected from the skull and stained with 4% triphenyl tetrazolium chloride (TTC, Sigma) 30min,  $37^{\circ}\text{C}$ . Images were obtained using commercial digital camera.

## **17. Intra-arterial cell injection**

24 hours after occlusion, right carotid bifurcation was re-exposed, and ZnMNP-NSCs ( $3 \times 10^6$  cells/ $100 \mu\text{l}$ ) were injected slowly ( $25 \mu\text{l}/\text{min}$ ) through carotid artery by use of polyethylene tube (Jeungdo, Seoul, Korea).<sup>42,43</sup>

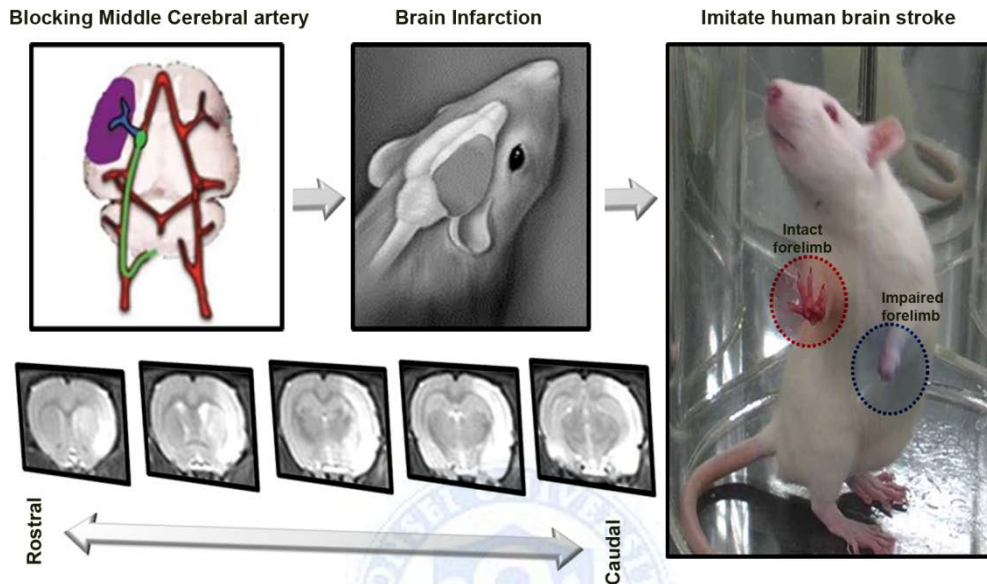


**Figure 1. Middle cerebral artery occlusion animal model.** Temporally blocking of middle cerebral artery imitate 80% of human brain stroke cases. As brain energy dependent processes fail, neurons are unable to maintain their normal transmembrane ionic gradients, resulting in an ion and water imbalance that leads to apoptotic and necrotic cell death cascades and ultimately the impairment of sensory and motor function.

## 18. Magnetic Resonance Imaging (MRI)

Both *in vitro* and *in vivo* MRI were performed by use of clinical 3.0 T MRI scanner (Achieva XT, Philips, Netherland) with animal coil (Shanghai Chenguang, China). Implanted neodymium was removed before scanning based on safety regulations of MRI. During the scanning, animals were anaesthetized with 2.5% isoflurane (Hana pharm) with oxygen. The T2 weighted images were obtained using in a fast spin echo sequence (TR/TE 4000 /80ms, field of view 50mm, matrix 256×256, slice thickness 0.5mm, acquisition number 1).<sup>18,44</sup>

The cerebral infarct volume in each brain were estimated using MRI. In T2-weighted images, infarction area reveal bright signal compared to intact area. MR images were obtained after cell injection 1-day, 1-week, 3-week. The results are expressed as percentage of infarct area compared with contralateral hemisphere area, considering that as 100%.<sup>45</sup>

## 19. Bioluminescence Imaging (BLI)

Some MCAO animals were transplanted ZnMNP-lenti-Fluc-GFP-NSCs with same condition.<sup>18,46</sup> Rats were given an intraperitoneal injection of D-luciferin (150mg/kg, Progenia, WI, USA). Animals were anaesthetized during the scan with 2.5% isoflurane (Hana pharm) with oxygen. BLI signal was recorded as maximum photon flux by IVIS spectrum *in vivo* preclinical imaging system (Perkin Elmer).<sup>18,46</sup> Living image 3.0

software (Perkin Elmer) was used to quantifying in the head.

**Table 4. Sequences of primers used for Quantitative RT-PCR**

<b>Gene</b>	<b>Gene Bank ID<sup>1</sup></b>	<b>Primers (5' → 3')<sup>2</sup></b>
<i>Nestin</i>	NM_006617	5'-GGCGCACCTCAAGATGTCC-3' 5'-CTTGGGGTCCTGAAAGGCTG-3'
<i>GFAP</i>	NM_001242376	5'-CTTCTCCAACCTGCAGATTCG-3' 5'-CACGGTCTTCACCACGATGTT-3'
<i>TUJ1</i>	NM_006086	5'-GGCCAAGGGTCACTACACG-3' 5'-GCAGTCGCAGTTTTTCACTC-3'
<i>GALC</i>	NM_001201401	5'-TCTCTGGGAGTCCATCTCTGC-3' 5'-CTACCACGTAGTGCCCACTCC-3'
<i>ZIC1</i>	NM_003403	5'-TGGCCCGGAGCAGAGTAAT-3' 5'-CCCTGTGTGCGTCCTTTTG-3'
<i>ZIC2</i>	NM_007129	5'-CACCTCCGATAAGCCCTATCT-3' 5'-GGCGTGGACGACTCATAGC-3'
<i>AXIN2</i>	NM_004655	5'-TACACTCCTTATTGGGCGATCA-3' 5'-TTGGCTACTCGTAAAGTTTT-3'
<i>Neurog2</i>	NM_024091	5'-CGCATCAAGAAGACCCGTAG-3' 5'-GTGAGTGCCCAGATGAGTTGTG-3'
<i>NEUROD1</i>	NM_002500	5'-ACCAAATCGTACAGCGAGAGT-3' 5'-CTCGTCCTGAGAACTGAGACA-3'
<i>GAPDH</i>	NM_001256799	5'-CCATGAGAAGTATGACAACAGCC-3' 5'-GGGTGCTAAGCAGTTGGTG-3'

<sup>1</sup> Query Genetic code of NCBI database ([www.ncbi.nlm.nih.gov/pubmed](http://www.ncbi.nlm.nih.gov/pubmed)).

<sup>2</sup> Primer sequences were obtained from the Primer bank database (<http://pga.mgh.harvard.edu/primerbank/>) and customized by Bioneer (Daejeon, Korea).

## **20. Assymmetric cylinder neurological test**

All animals underwent behavioral tests before MCAO and 1, 7, 21 days after transplantation. This test was used to evaluate locomotor asymmetry.<sup>47,48</sup> As the animal moved within an open-top, clear plastic cylinder (diameter 200 mm, height 300 mm) in front of 2 mirrors those are arranged as right angles. Forelimb activity while rearing against the wall of the cylinder is recorded for 10 minutes. The results were expressed as percentage of impaired forelimb activity compared with total forelimb activity.

## **21. Statistical analysis**

The statistic software SPSS18.0 (SPSS Inc., Chicago, IL, USA) was used for data analysis. Values were reported as mean±SEM. Statistical differences were assessed either by a non-parametric Mann-Whitney U test and a non-parametric one-way Kruskal-Wallis test. A value of  $p < 0.05$  was chosen for statistical significance.

## **22. Code of ethics and law**

All *in vitro* experiments were conducted in level 2 LMO (living modified organism) facility. Quantitative real-time reverse transcription-polymerase chain reaction was

followed according to the MIQE (minimum information for publication of quantitative real-time PCR experiments) guideline. All animal experiments were conducted in SPF (specific pathogen free) facility received full accreditation by AAALAC international and complying the previous ethical guideline. The ARRIVE (animal research : reporting *in vivo* experiments) guideline was considered in the design and report of the study.

### **III. RESULTS**

#### **1. Human neural stem cells form self-renewing neurospheres and have multipotency**

Proliferating single cells from the telencephalon of human fetus at 13 weeks of gestation (termed NSCs) give rise to free-floating spheres called neurospheres; These were identified by their phase-bright appearance (Fig. 2 a).<sup>19</sup> To analyze the cellular composition of the neurosphere, we investigated the expression of lineage specific markers. Most of neurosphere forming cells (95-99%) express Pax6, Nestin, Sox2, CD133, PCNA, KI67, GFAP, vimentin (Fig. 2 b-e) known as immature markers. Some cells that strongly expressed Tuj1 were predominantly found in the sphere core (Fig. 2 f). Also, neurosphere forming cells express and secrete several neurotrophic factors such as neurotrophin-3 (NTF3; Fig. 2 g), neurotrophin-4 (NTF4; Fig. 2 i), brain-derived neurotrophic factor (BDNF; Fig. 2 j), nerve growth factor (NGF; Fig. 2 h), glial-derived neurotrophic factor (GDNF; Fig. 2 k), vascular endothelial growth factor (VEGF; Fig. 2 l), fibroblast growth factor (FGF; Fig. 2 m). When plated on PLL coated dish without mitogen, NSCs expressed Tuj1 as an early neuron marker (Fig. 2 o), glutamate as a glutamergic interneuron marker (Fig. 2 p), Calretinin as a GABAergic interneuron marker (Fig. 2 q), TH as a dopaminergic neuron (Fig. 2 r). GFAP and S100- $\beta$  as astroglial markers (Fig. 2 s,t), MBP and O4 as oligodendrocytic markers (Fig. 2 u,v). These data confirm that our NSCs are capable of self-renewing and multipotent under differentiation conditions.<sup>49-51</sup>

## 2. Firefly luciferase expressing neural stem cells

NSCs were exposed to lentiviral particle including Fluc gene and reporter gene GFP

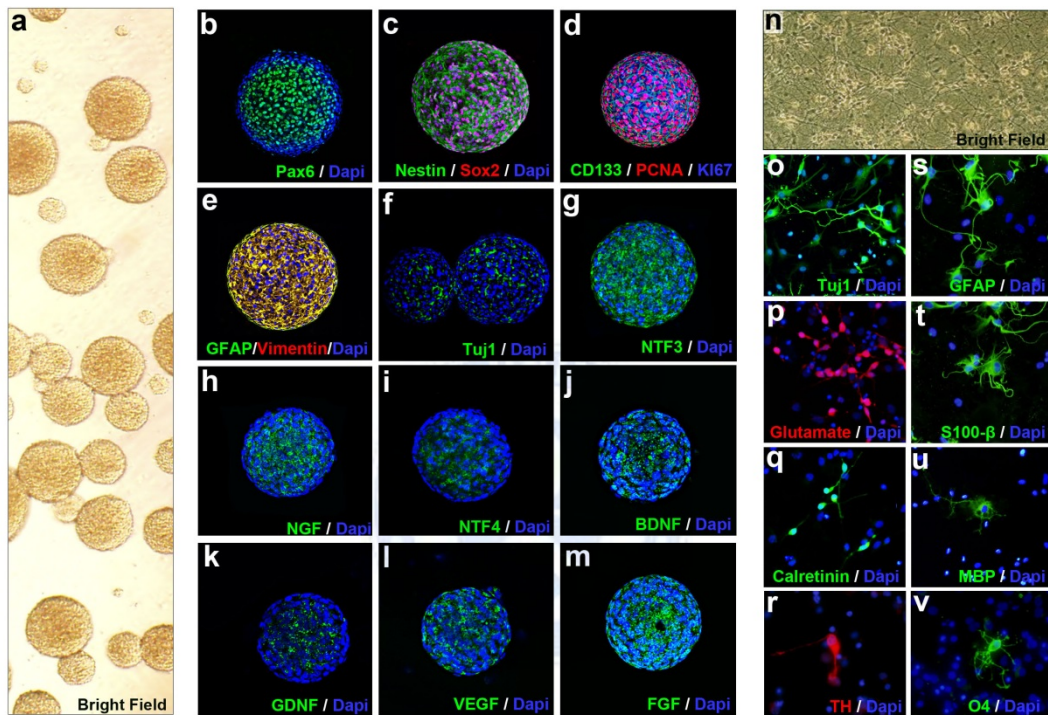


**Figure 2. Neural stem cell characterization.** (a-m), Neurosphere formation by proliferating neural stem cells. Phase microscopy (a) and immune fluorescence labeling (b-m) of representative telencephalic neurosphere grown in bFGF and LIF. Neurospheres were stained for Pax6 (b), Nestin with Sox2 (c), CD133 with PCNA (d), GFAP with Vimentin (e), Tuj1 (f), NTF3 (g), NGF (h), NTF4 (i), BDNF (j), GDNF (k), VEGF (l), FGF (m). Under differentiation conditions, neural stem cells differentiated into multiple lineages. Phase microscopy (n), neuronal markers (o-r) and astroglial markers GFAP (s) and S100- $\beta$  (t) were shown. A few cells expressed oligodendrocyte markers MBP (u) and O4 (v).

(Fig. 3 a). Fluc gene expressing cells produced near-infrared photon signaling in the presence of D-luciferin (Fig. 3 b<sub>i</sub>, b<sub>ii</sub>). Only GFP not Fluc expressing cells were not produce signal (Fig. 3 b<sub>iii</sub>). Flow cytometry confirmed that 93.1% of NSCs expressed foreign gene (Fig. 3 d). Lentiviral Fluc expressing NSCs (Lt-Fluc-NSCs) formed neurosphere as well as original NSCs (Fig. 3 d). The Fluc activity continuously increased in NSCs in proportion to cell number (Fig. 3 e). Using these characteristics, Lt-Fluc-NSCs were used to visualize the cellular location and to measure of the number of cells.

### 3. Zn-doped magnetic nanoparticle properties and intracellular labeling

ZnMNP was designed into three multiple layers (Fig. 4 a). Central core was the source of strong magnetic properties. Inner layer was dextran for biocompatibility, surface layer was PLL for cell transfection. Due to the three-layer structure, ZnMNP had high magnetic saturation magnetization (161 emu/g; Fig. 4 b), equally contributed in circular form of 18nm diameter scale (Fig. 4 c, d) and easily transfected to NSCs. In Prussian blue staining, more than 95% cells showed cytosolic nanoparticles (Fig. 4 e, f). Inductively Coupled Plasma (ICP) analysis revealed that  $4.58 \pm 0.94$  pg of ZnMNP was internalized in single neural stem cells. In electron microscope image, cytosolic nanoparticles were settled in endosomal vesicles (Fig. 4 g, h). Ferumoxide (FeMNP) often used to labeling cells<sup>52</sup> but FeMNP had lower magnetization (105 emu/g; Fig. 4 b). FeMNP labeled cells could be detected by MRI at least 50,000 cells per 1 mm<sup>3</sup>. By contrast, ZnMNP cells were detected in 1,000 cells per 1 mm<sup>3</sup> (Fig. 4 i, j).



In order to examine whether the ZnMNPs were decomposed inside the NSCs, fluorescence zinc ion indicator (Fig. 5 a) was used. Both flow cytometry (Fig. 5 b) and fluorescence images (Fig. 5 c) showed no difference. These data suggest that NSCs were not exposed to over concentration of Zn ion.

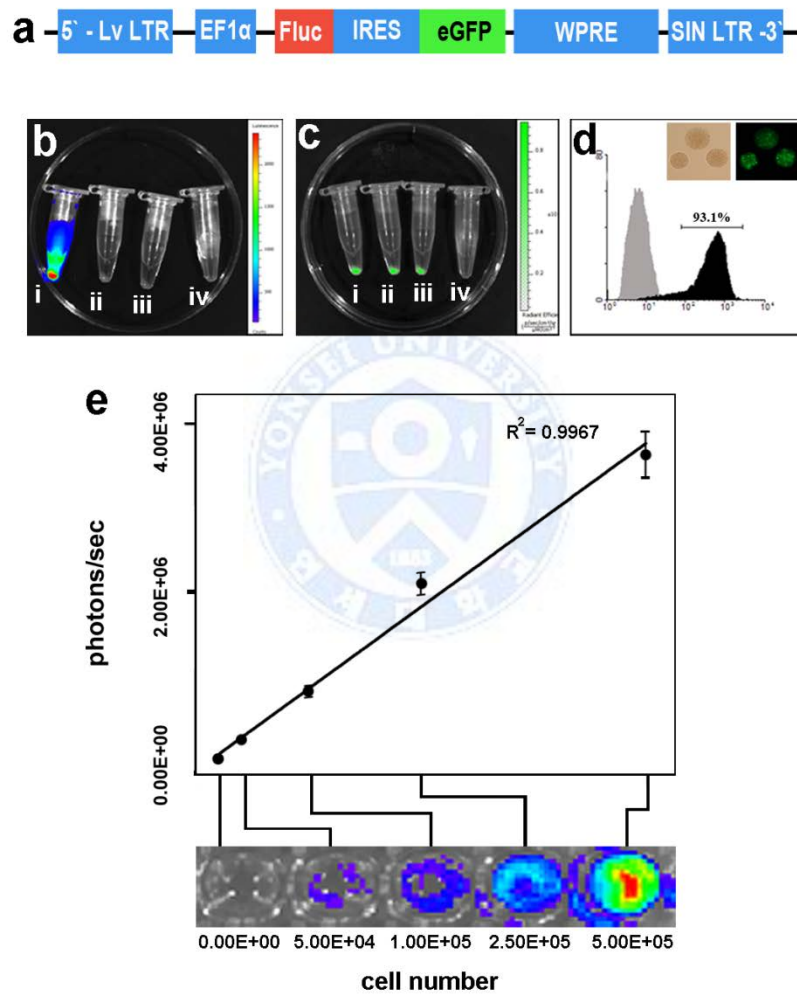


**Figure 3. Firefly Luciferase and GFP expressing NSCs.** (a), Recombinant lentiviral vector containing Fluc and GFP. (b), Fluc and GFP expressing NSCs produced near-infrared signaling in the presence of D-luciferin (b<sub>i</sub>). In the absence of D-luciferin, signal

was not detected (**b<sub>ii</sub>**). Only GFP expressing cells, signal was not detected in the presence or absence of D-luciferin (**b<sub>iii</sub>**). (**d**), 93.1% of total cells express Fluc and GFP in flow cytometry. Fluc and GFP expressing cells formed neurosphere as well as non-transfected NSCs. (**e**), Fluc activating signal was directly proportional to stem cell number.

#### **4. Magnetotactic ability of Zn-doped magnetic nanoparticle-neural stem cells**

The attraction force ( $F_m$ ) of ZnMNPs, which serves as an engine of the ZnMNP-NSCs, depends on the magnetic gradient field of magnet ( $F_m = V(M \cdot \nabla)B$ ), where  $V$  is volume of MNP;  $M$  is magnetization value of MNP;  $B$  is magnetic gradient field).<sup>53</sup> According to the simulation study (Fig. 6 a), the attraction force experienced by the single ZnMNP-NSC under the magnetic gradient field of typical NdFeB magnet was increased from 2 pN to 170 pN as the distance between the magnet and ZnMNP-NSCs is decreased from 1 cm to 0 cm. Considering the diameter of rat brain is less than 1 cm, entire rat brain can be exposed under adequate magnetic gradient field by placing the magnet on head. Thus, ZnMNP-NSCs transplanted to the rat brain are expected to have attraction force of pico-Newton range which is known to promote the displacement of the cells.<sup>54-57</sup> To demonstrate the ability of the magnet-guided delivery of ZnMNP-NSCs, we choose rat brain as a model system. Prior to performing *in vivo* experiment, we first tested magnet-guided delivery in a brain mimicking *in vitro* model (Fig. 6 a). This model consists of two different compartments; one is 0.2 % (wt/v) agarose gel which is known to have similar density with brain tissue,<sup>27</sup> the other is capillary tube containing phosphate buffer saline (PBS) which mimics the blood vessel environment. For visualization of the cell migration,

NSCs were labeled with luciferase that can be detected using bioluminescence imaging (BLI). Three groups of cells (ZnMNP-NSCs, FeMNP-NSCs, and NSCs) were loaded to the capillary tube and exposed to the magnetic field (1.0 Tesla NdFeB magnet). After applying magnetic field for 12 hours, ZnMNP-NSCs migrated toward the magnet penetrating the agarose gel. In the case of FeMNP-NSCs, cells migrated toward the magnet but they did not penetrate the gel. Non-labeled NSCs were somewhat diffused in

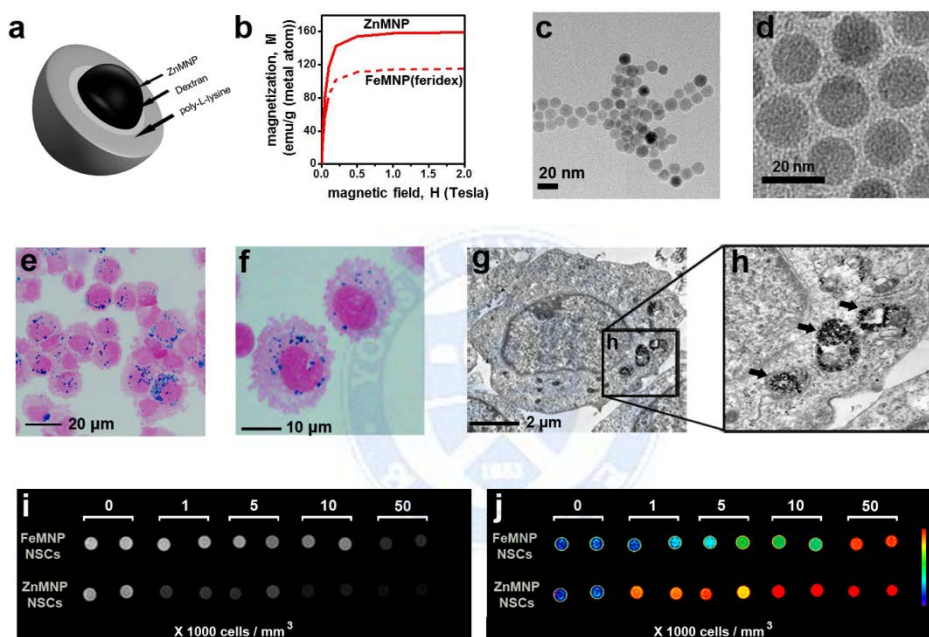


**Figure 4. Zn-doped magnetic nanoparticle and intracellular labeling.** (a), Tri-layer structure of ZnMNP. (b), Magnetic power of ZnMNP compared to commercial particle. (c, d), Transmission electron microscope image of ZnMNP. (e, f), Perl's prussian blue staining with nuclear fast red counter staining of ZnMNP labeled NSCs. (g, h), Transmission electron microscope image of ZnMNP labeled NSCs. (i, j), In vitro phantom MR image of commercial particle and ZnMNP labeled NSCs.

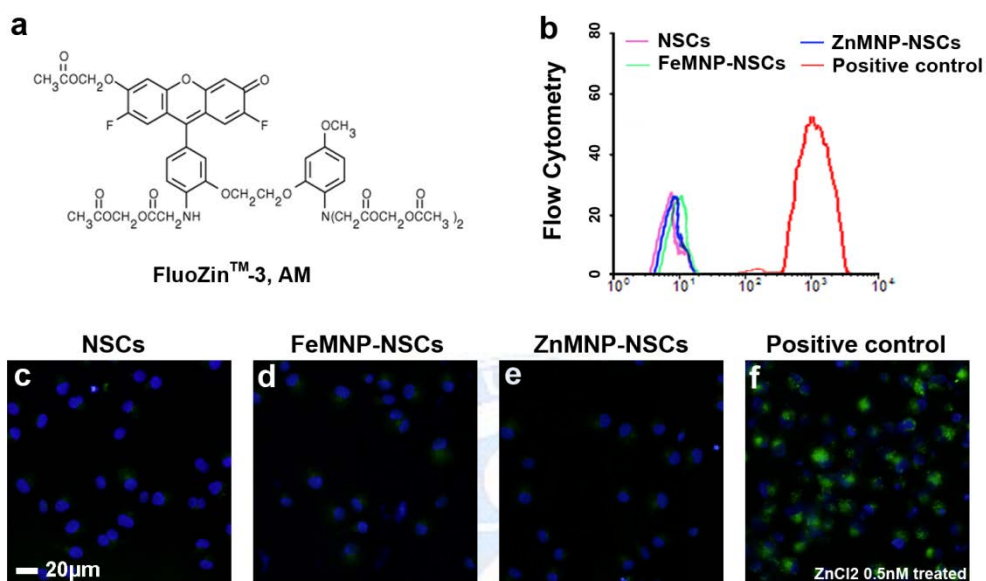


**Figure 5. Zinc ion staining.** (a), Chemical structure of Zinc ion indicating fluorescence dye. For the positive control, 0.5nM ZnCl<sub>2</sub> was treated. NSCs, FeMNP-NSCs and ZnMNP-NSCs shows no difference in flow cytometry (b) and microscopic observations (c-f).

the capillary but did not reach to agarose gel region (Fig. 6 c). These results indicate that only ZnMNP-NSCs possess sufficient magnetic attraction force for magnet-guided delivery in rat brain.

To gain further evidence for the magnetotaxy of ZnMNP-NSCs, *in vivo* magnetic guidance experiment was performed using rat. ZnMNP-NSCs were transplanted in subventricular zone (SVZ) of rat brain and magnetic gradient field was applied by attaching NdFeB magnet on the head of rat (Fig. 7 f). The location of the transplanted ZnMNP-NSCs was non-invasively monitored using magnetic resonance imaging (MRI) in the adult rat brain. In general, transplanted NSCs into the SVZ migrate toward the left olfactory bulb (OB) *via* a route called the rostral migratory stream (RMS), and along the corpus callosum (CC) and white matter tract (WM) in response to normal microenvironmental cues (Fig. 7 a-c).<sup>58</sup> Using magnetic guidance, it is possible to change the migration route as desired. ZnMNP-NSCs were transplanted into SVZ of the adult rat brain and exposed to magnetic field for 7 days, cells migrated toward the magnet positioned at the upper region of the brain cortex (Fig. 7 d-g). The results clearly demonstrate that the migration of ZnMNP-NSCs can be effectively controlled using a magnet in an *in vivo* system.

## **5. Effects of Zn-doped magnetic nanoparticle in neural stem cell homeostasis**

We studied the biocompatibility and effects of ZnMNP on NSCs. According to a dosage-dependent cell viability test, ZnMNP induce no toxic effects even at the high concentration of 1000 (Fe)  $\mu\text{g/ml}$  (Fig. 8 a) and after long-term exposure (Fig. 8 b). Additionally, there were no significant changes in both TUNEL staining (Fig. 8 c) and

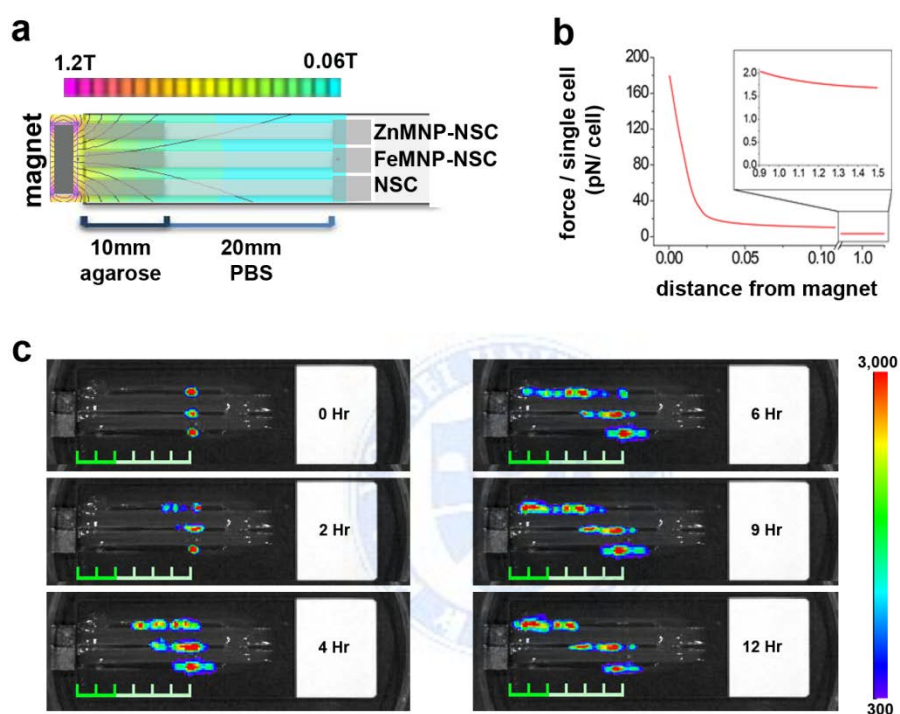


**Figure 6. *In vitro* magnetotactic migration.** (a), Brain mimicking *in vitro* model. 0.2% agarose gel which is known to have similar density with brain tissue. (b), The amount of the magnetic attraction force of single cell according to the distance from magnet. (c), Magnetic guided migration of NSCs, FeMNP-NSCs, ZnMNP-NSCs in brain mimicking *in vitro* system.

『Abbreviation』 T; tesla.

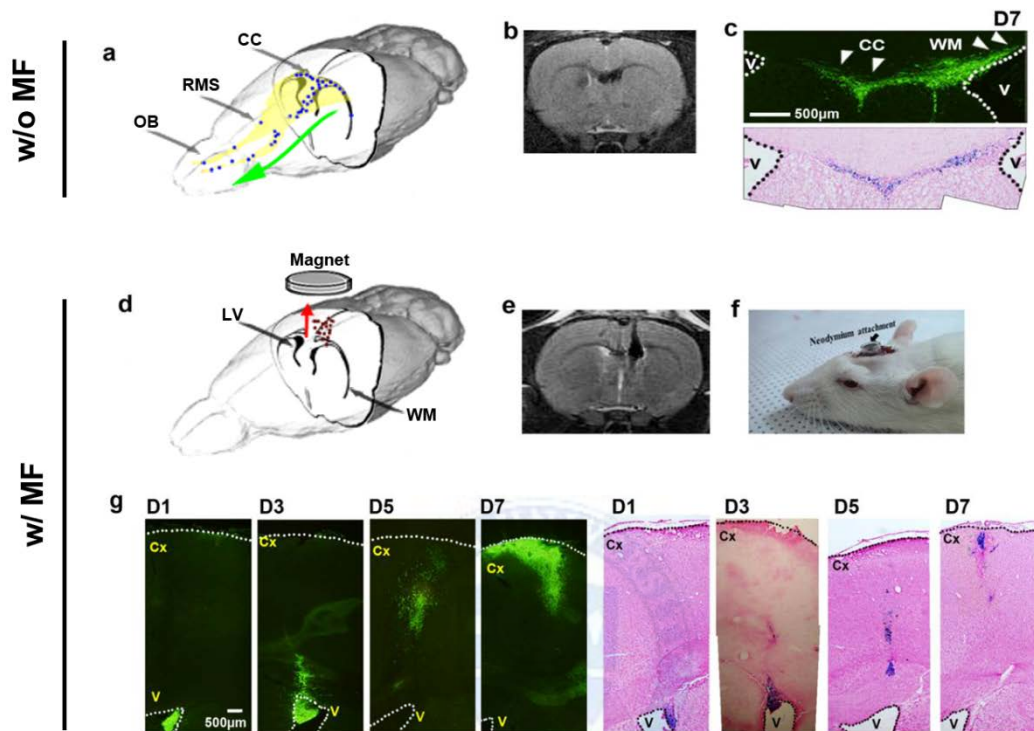


**Figure 7. *In vivo* magnetotactic migration.** (a), Without magnetic field, cells migrated via rostral migratory stream (RMS, blue dots). (b,c), MR image and histological images showed migrating path of non-magnet guided migration via RMS. (d), In a static magnetic field, cell migrating route was changed (red dots). (e), MR image showed altered migrating path. (f), Magnet attachment of animal skull bregma. (g), Histological images showed altered migrating path with the temporal scale of day1, day3, day5, day7.

『**Abbreviation**』 w/o MF; without magnetic field, w MF; with magnetic field, LV; lateral ventricle, cc; corpus callosum, OB; olfactory bulb, RMS; rostral migratory stream, WM; white matter tract, Cx; cerebral cortex, V; Ventricle, D; days post transplantation

active-caspase3 immunocytochemistry (Fig. 8 d). These data suggest that there were no toxic effect of ZnMNP on NSCs.

Caveat may arise of oxygen free radical production or genotoxicity. However, there were no significant difference of reactive oxygen species level (Fig. 9 b) and showed no DNA disruption (Fig. 9 c-f)

There were no changes in neurosphere morphology such as marker expression (Fig. 9 a-c), neurosphere number (Fig. 10 d), NSCs number (Fig. 10 e), NSCs number per single neurosphere (Fig. 10 f), neurosphere diameter (Fig. 10 g).

To the next, we analyzed the proliferation of ZnMNP-NSCs compared with NSCs and FeMNP-NSCs. Pre-treated 2 $\mu$ M BrdU was immunelabeled and counted by flow-cytometry (Fig. 11 b) and observed by microscope (Fig. 11 c-e). There were no significant changes in the proliferation.

## 6. Neuronal differentiation of ZnMNP-NSCs

In genetic screening by use of PCR, gene expression pattern was changed. Basic helix loop helix (bHLH) proneural transcription factors (*NEUROGENIN-2*, *NEUROD1*, *ASCLI*) and neuronal gene (*TUJ1*, *SCG10*, *TBR2*) were increased in ZnMNP-NSCs compared to control groups (Fig. 12 a). Similarly, the differentiation patterns of ZnMNP-NSCs were significantly different from those of unlabeled NSCs and FeMNP-NSCs. In the case of the ZnMNP-NSCs, neuronal differentiation was markedly increased under the differentiation condition. The percentage of neuronal marker Tuj1 positive cells in



ZnMNP-NSCs were significantly increased compared to NSCs and FeMNP-NSCs *in vitro* (Fig. 12 j-l,n, Table. 5) while neural stem cell marker nestin and glial marker GFAP were decreased (Fig. 12 b-d, f-h, n, Table. 5). Additionally, the treatment of Wnt signal

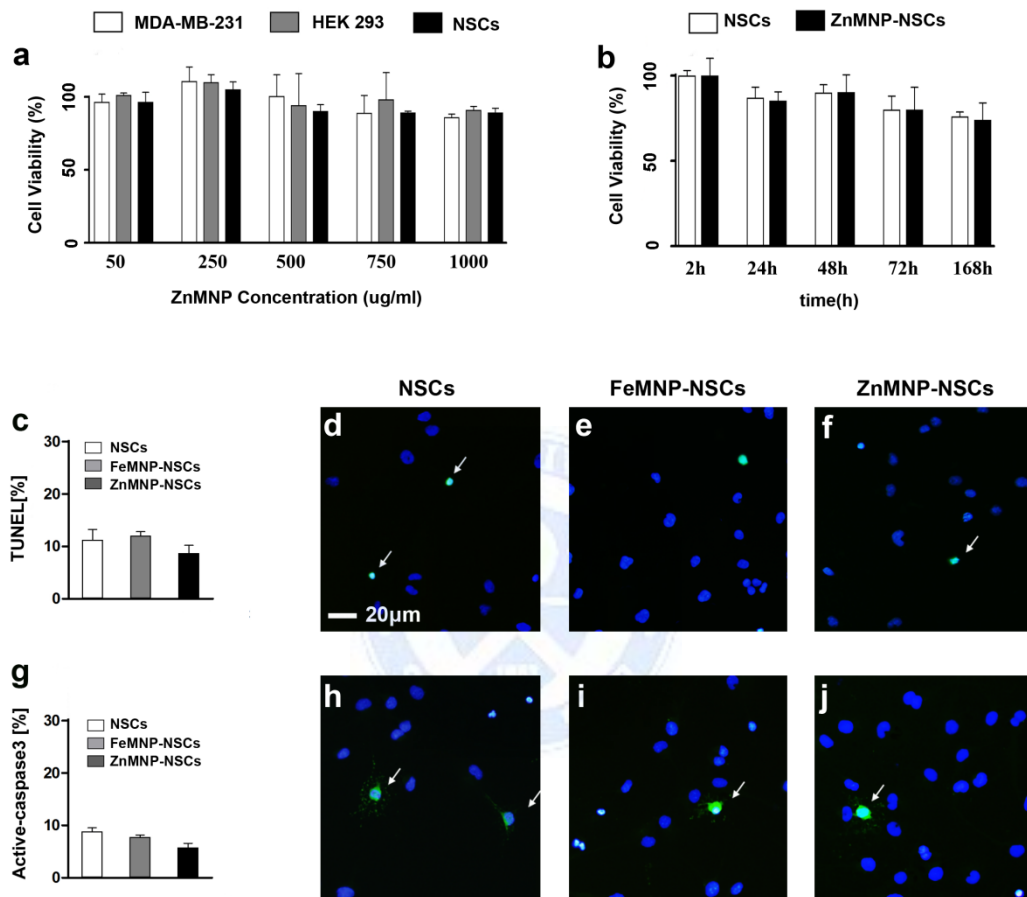


**Figure 8. Zn-doped magnetic nanoparticle mediated apoptosis.** (a), Mitochondrial function of NSCs according to the ZnMNP concentrations. No significant changes among three groups. (b), Mitochondrial function of long term exposure of ZnMNP to NSCs. No significant changes between two groups. (c-j), TUNEL staining and active caspase-3 immuno cytochemistry shows no difference among three groups. All data were expressed as mean±Standard error of the mean (SEM).

『Abbreviation』 TUNEL; terminal deoxynucleotidyl transferase dUTP nick and labeling

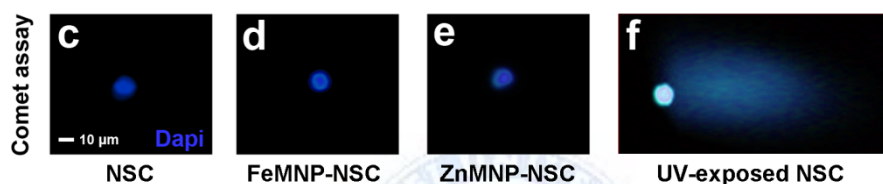
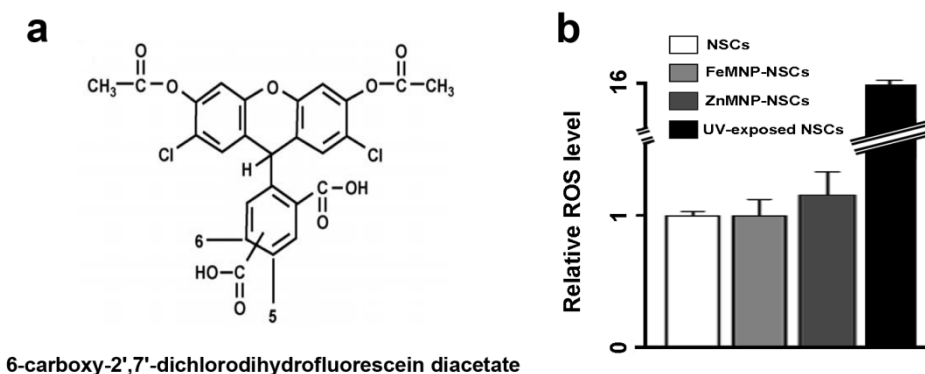


**Figure 9. Zn-doped magnetic nanoparticle mediated genotoxicity.** (a), Chemical structure of ROS indicating dye. (b), ROS level shows no difference among three groups. For the positive controls, NSCs were exposed ultraviolet 20 minutes and ROS level was enormously increased. (c-f), Comet assay to determine the genotoxicity. Comet tail seems to occur if the genomic DNA was fragmented. UV-exposed NSCs showed typical fragmented genomic DNA in Dapi staining (f). All three groups showed no genotoxicity. All data were expressed as mean±SEM.

『Abbreviation』 ROS; reactive oxygen species, UV; ultra-violet

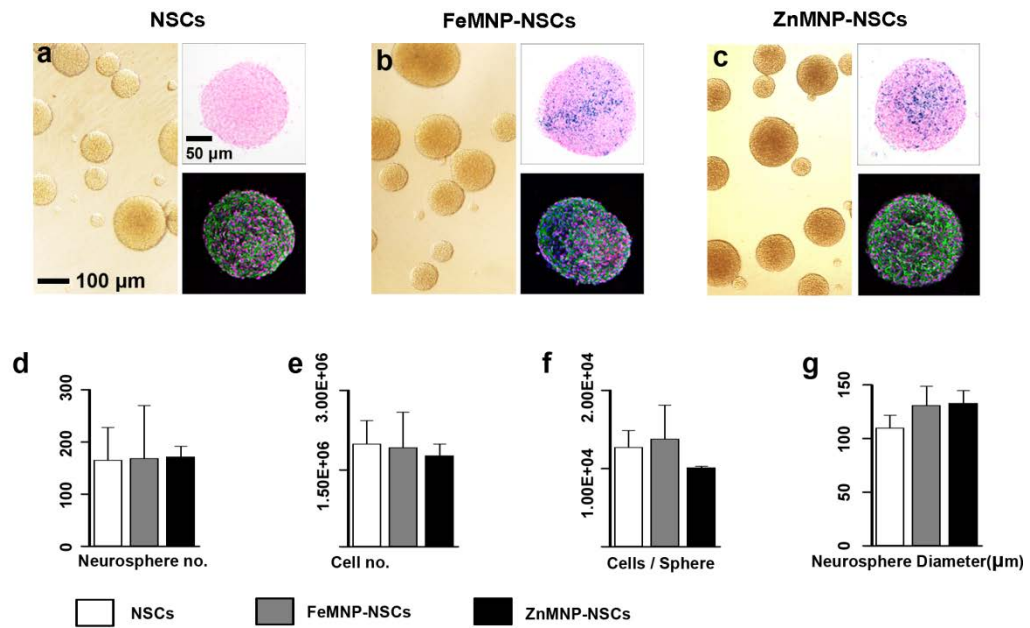


**Figure 10. Neurosphere assay.** (a), Non-labeled neural stem cells formed neurosphere. (b), FeMNP-labeled neural stem cell formed neurosphere. (c), ZnMNP-labeled neural stem cell formed neurosphere. (d-g), Neurosphere morphologies. All data were expressed as mean±SEM.

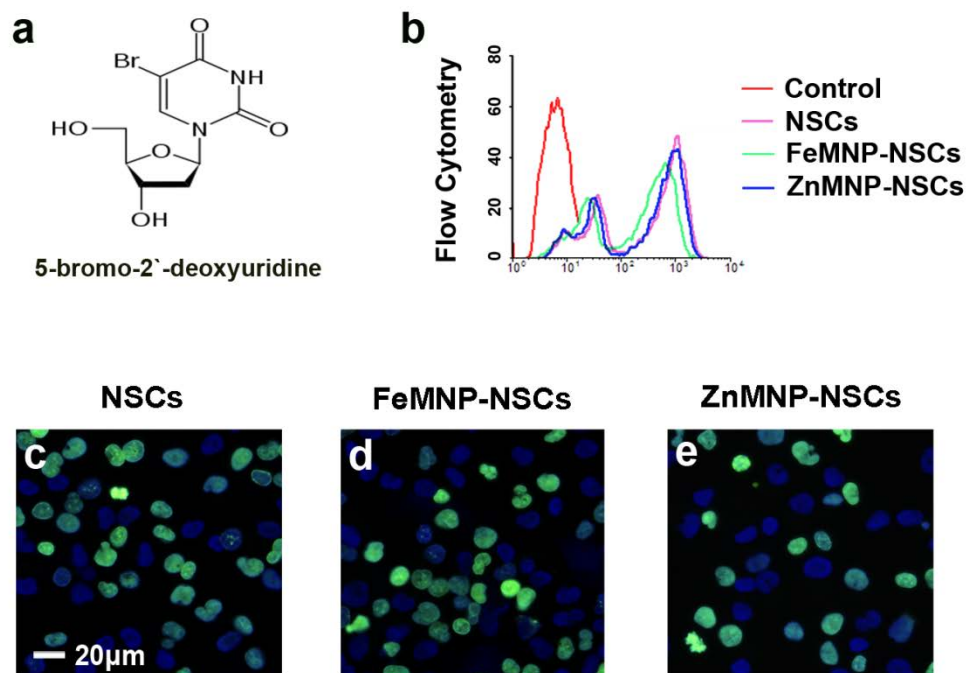


**Figure 11. BrdU proliferation assay.** (a), Chemical structure of BrdU. (b), Flow cytometry of BrdU positive cells. No significant changes among three groups. (c-e), Immunocytochemistry of BrdU-proliferating cells.

blockade Dickkopf1 (DKK1) into ZnMNP-NSCs (ZnMNP-NSCs-DKK1) reduced the effect of ZnMNP on promoting neurogenesis and repressing gliogenesis of NSCs (Fig. 12 e,i,m,n, Table. 5), which strongly suggest that the Wnt signaling is involved in the neuronal differentiation of ZnMNP-NSCs

In order to ensure the involvement of Wnt signaling pathway, we tracked cellular location of  $\beta$ -catenin. Immunohistochemistry against  $\beta$ -catenin shows translocation of  $\beta$ -catenin in the presence of ZnMNP (Fig. 13 e-h). Non-labeled NSCs's  $\beta$ -catenin were located in cytoplasm attached to the cell nucleus (Fig. 13 a-d). Also, Reporter assay was conducted. ZnMNP labeled cells were showed increased TCF/LEF promoter activation (Fig. 13 i-j). TCF/LEF promoter was activated when Wnt signaling mechanism was activated.

Western blotting analysis and quantitative real time PCR (Q-PCR) analysis were conducted. Q-PCR analysis revealed zinc finger of the cerebellum1 (*ZIC1*) and zinc finger of the cerebellum2 (*ZIC2*) increment in ZnMNP-NSC *in vitro* (Fig. 14 c). Interestingly, *ZIC* transcription factors were increased whether DKK1 was present or not (Fig. 14 c). This data suggest that *ZIC1*, *ZIC2* were located in the middle of the pathway; downstream of ZnMNP and upstream of wnt signaling pathway. In western blot analysis, Wnt ligands (Wnt1, Wnt3a) were increased both in cell culture media (Fig. 14 a) and cell lysate (Fig. 14 b).  $\beta$ -catenin, the key molecule of wnt signaling pathway, was less decomposed in ZnMNP-NSC compared to controls (Fig. 14 b). *AXIN2*, representative wnt signaling reporter gene which was measured by Q-PCR, was increased in ZnMNP-NSC compared to controls (Fig. 14 c). Treating DKK1, both  $\beta$ -catenin and *AXIN2* level were neutralized from ZnMNP's influence (Fig. 14 b, c). Indeed, proneural bHLH transcription factors (*NEUROGENIN-2*, *NEUROD1*), neuronal gene (*TUJ1*), neuronal proteins (Tuj1, Map2) were increased in ZnMNP-NSCs and reduced by DKK1 (Fig. 14 b,c). These data suggest that ZnMNP increases *ZIC1*, *ZIC2* expression, then secrete wnt ligands (Wnt1, Wnt3a), continually activate canonical wnt signaling pathway resulting proneural bHLH transcription factor (*NEUROGENIN-2*, *NEUROD1*) increment.

Ultimately, neuronal markers (*TUJ1*, Tuj1, Map2) increment appeared. Also, ZnMNP-NSCs showed augmented of nerve growth factor (NGF), neurotrophin factor-3 (NTF3) secretion compared to controls (Fig. 14 a). Neural stem cell neurogenesis mediated by ZnMNP mechanism was summarized in the Fig. 15. Next, we confirmed that neurogenic phenomenon *in vivo*. We transplanted ZnMNP-NSCs (or controls; NSCs,

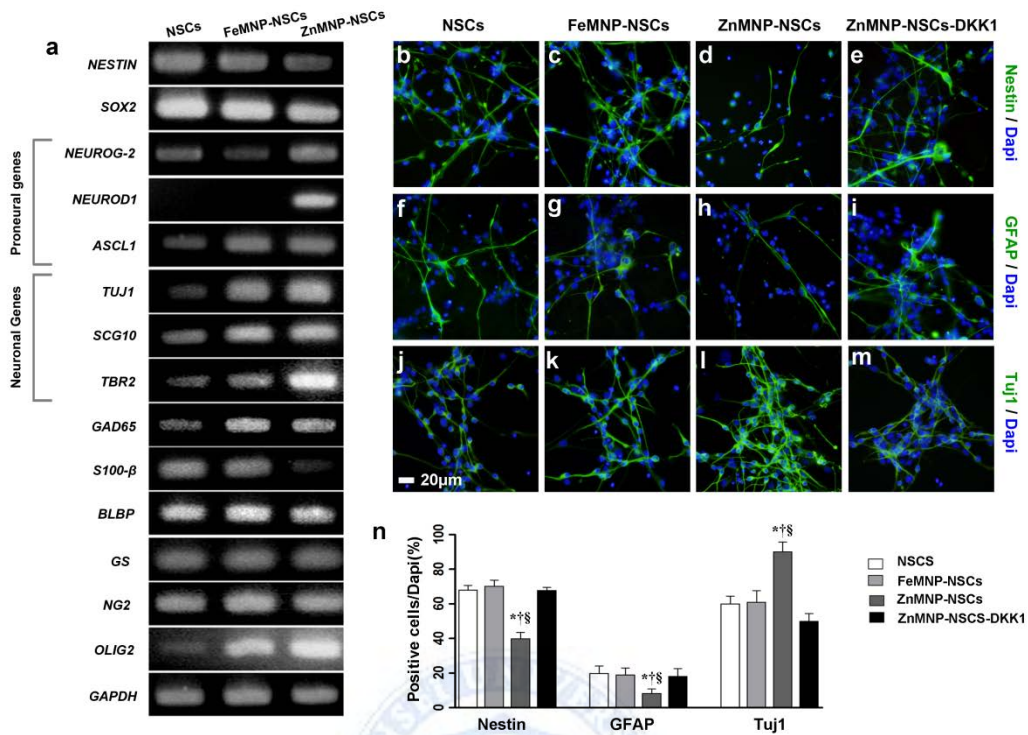


**Figure 12. Genetic screening and differentiation patterns *in vitro*.** (a), Traditional PCR analysis of ZnMNP-NSCs. Proneural bHLH transcription factors and neuronal genes were increased. (b-e), NSCs` marker Nestin expression of ZnMNP-NSCs and control groups. (f-i), Glial marker GFAP expression of ZnMNP-NSCs and control groups. (j-m), Neuronal marker Tuj1 expression of ZnMNP-NSCS and control groups. ZnMNP-NSCs showed increased neuronal differentiation and decreased self renewing and glial differentiation. All changes were neutralized by DKK1 (b-n). All data were expressed as mean±SEM. \*p<0.05 compared to NSCs, †p<0.05 compared to FeMNP-NSCs, §p<0.05 compared to ZnMNP-NSCs-DKK1.

『Abbreviation』 ASCL1; ,Neurog2; neurogenin2

**Table 5. Differentiation pattern of Zn-doped magnetic nanoparticle-neural stem cells *in vitro* and *in vivo***

		NSCs (n=3)	FeMNP- NSCs (n=3)	ZnMNP- NSCs (n=3)	ZnMNP- NSCs-DKK1 (n=3)
<i>In vitro</i> <sup>1</sup>	<b>Nestin</b>	60.24±2.15	70.35±3.34	40.00±3.51 <sup>*†§</sup>	52.00±1.59
	<b>GFAP</b>	20.00±4.00	19.20±3.77	8.34±2.45 <sup>*†§</sup>	18.32±4.24
	<b>TUJ1</b>	60.24±4.24	61.23±6.42	90.36±5.32 <sup>*†§</sup>	50.18±4.21
<i>In vivo</i> <sup>2</sup>	<b>Nestin</b>	74.17±0.96	86.83±0.44	72.53±3.97	
	<b>GFAP</b>	49.78±9.83	60.20±8.90	48.67±10.17	
	<b>TUJ1</b>	11.9±3.42	13.66±3.23	39.52±7.38 <sup>*†</sup>	

<sup>1</sup> *In vitro* experiments, data were expressed as a percentage of the Dapi-positive cells.

<sup>2</sup> *In vivo* experiments, data were expressed as a percentage of the hNuc-positive cells.

All data were expressed as mean±SEM. \* p<0.05 compared to NSCs, † p<0.05 compared to FeMNP-NSCs, § p<0.05 compared to ZnMNP-NSCs-DKK1.

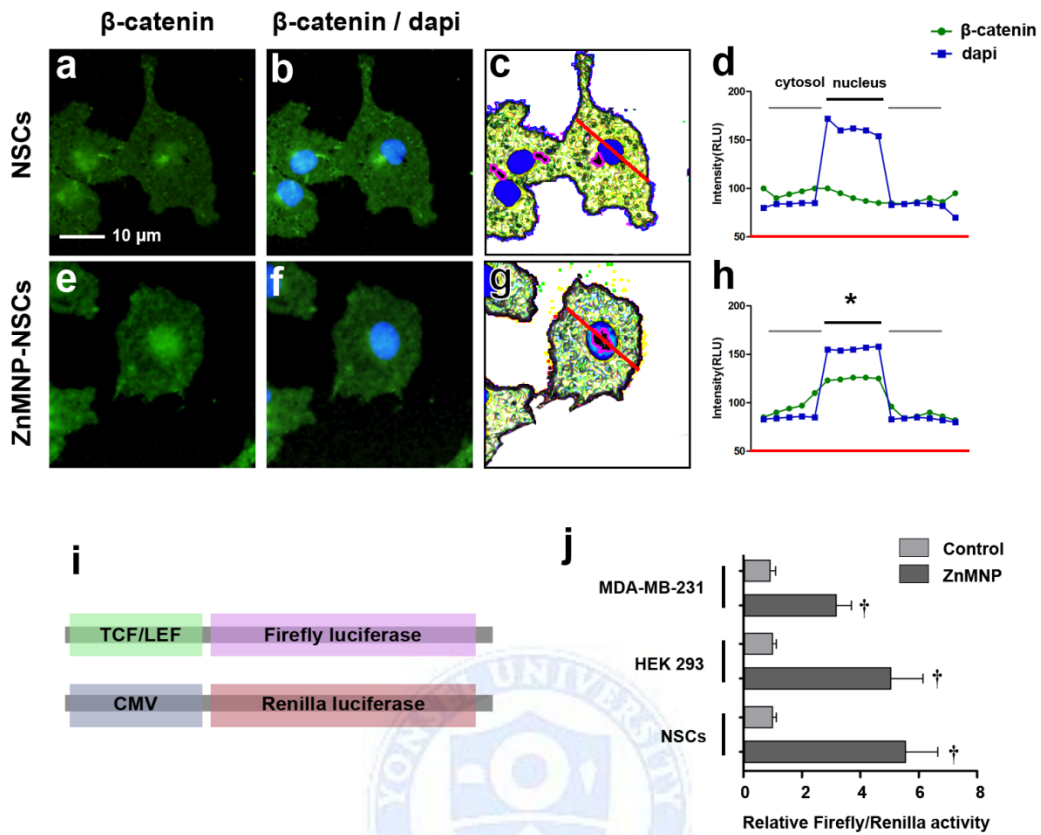


**Figure 13. Zn-doped magnetic nanoparticle mediated activation of Wnt signaling pathway. (a-h),** Nuclear trans-location of  $\beta$ -catenin. NSCs exhibit cytosolic  $\beta$ -catenin (a-d). By contrast, ZnMNP-NSCs showed nuclear positioned  $\beta$ -catenin (e-h). (i), Reporter assay plasmid construction. TCF/LEF promoter is activated only in the activated Wnt signaling pathway cause expression of firefly luciferase. CMV promoter is housekeeping promoter. (j), MDA-MB-231 cells and HEK 293 cells exhibit ZnMNP mediated wnt signaling activation as with the neural stem cell. All data were expressed as mean $\pm$ SEM (n=3). \* Overlapping areas of  $\beta$ -catenin and Dapi, <sup>†</sup>p<0.05 compared to control.



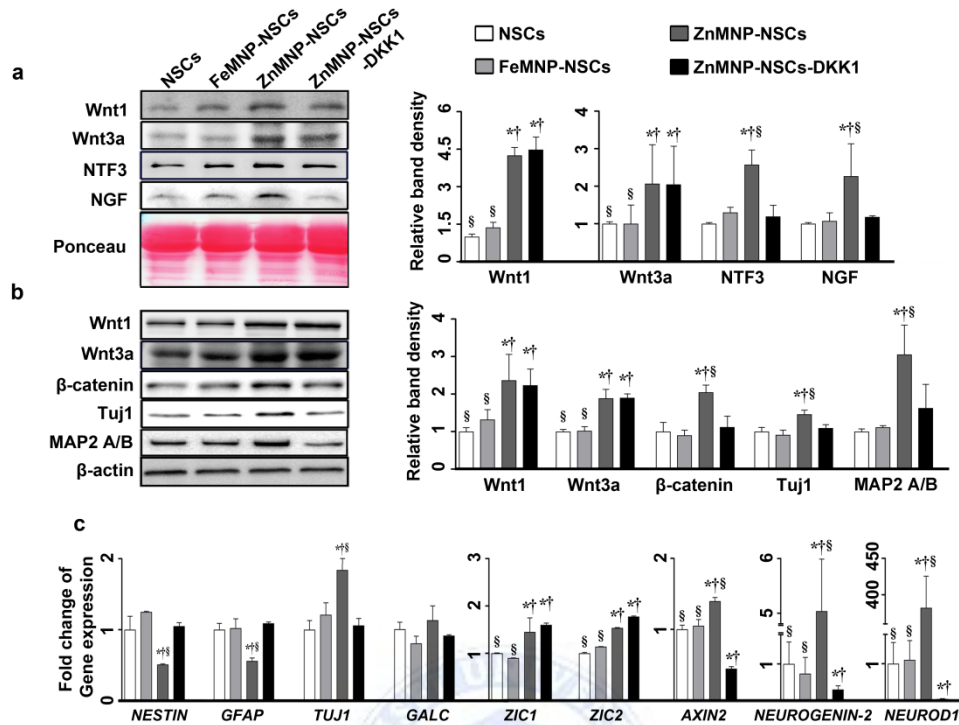


**Figure 14. Western blot analysis and Quantitative polymerase chain reaction analysis.** (a), Relative levels of Wnt1, Wnt3a, NTF3, NGF using western blot analysis in cell culture medium of NSCs, FeMNP-NSCs, ZnMNP-NSCs, ZnMNP-NSCs-DKK1. (b), Relative levels of Wnt1, Wnt3a, β-catenin, Tuj1, MAP2 A/B using western blot analysis in the cell lysates. (c), The relative expression of mRNA for *NESTIN*, *GFAP*, *TUJ1*, *GALC*, *ZIC1*, *ZIC2*, *AXIN2*, *NEUROG-2*, *NEUROD1*. All data represent mean ± SEM (n=3), \*p<0.05 compared to NSCs, †p<0.05 compared to FeMNP-NSCs, §p<0.05 compared to ZnMNP-NSCs-DKK1.

『Abbreviation』 Neurog2; neurogenin2

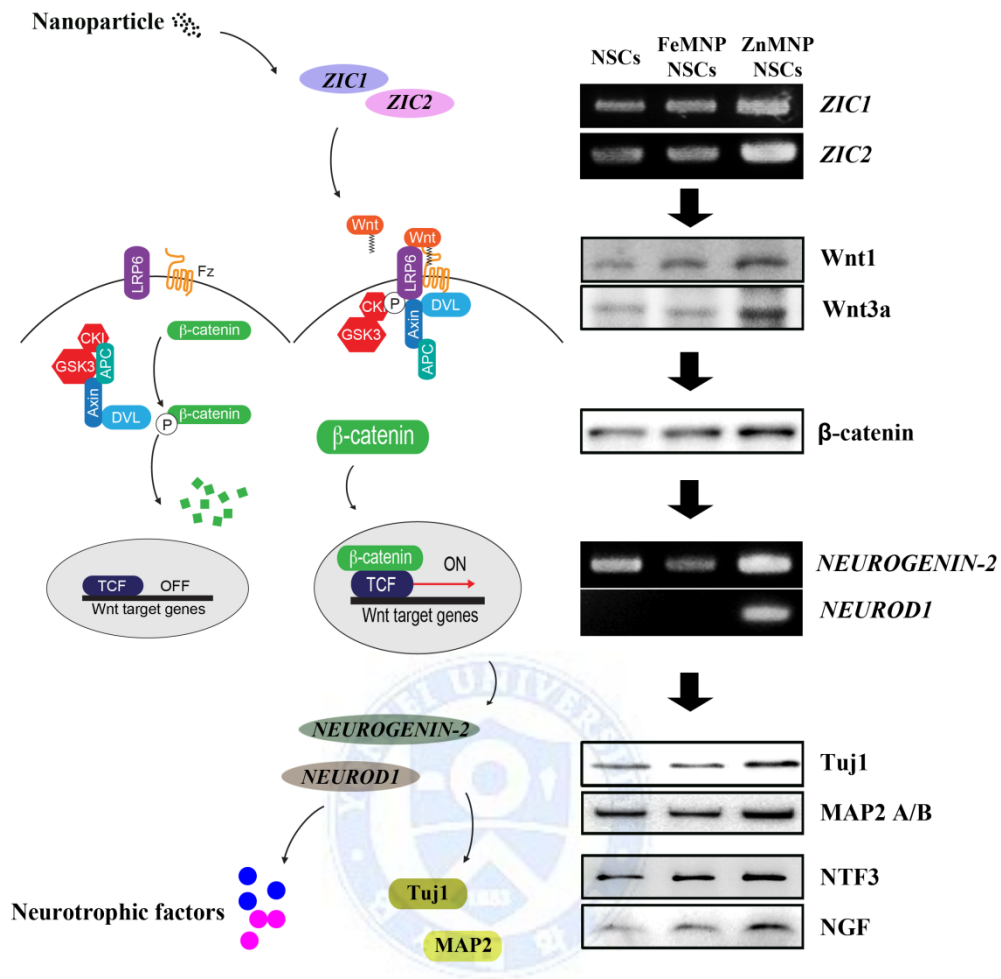


**Figure 15. Mechanism of Zn-doped magnetic nanoparticle mediated neural stem cell neurogenesis.** Foremost, *ZIC1*, *ZIC2* transcription factors were increased. Like *Xenopus* system, *ZIC* transcription factors induce the secretion of *Wnt1*, *Wnt3a* ligands. Through the canonical wnt signaling pathway,  $\beta$ -catenin level was increased and translocated to cell nucleus. Wnt target genes, *NEUROGENIN-2*, *NEUROD1*, reponse to the signal and force neurogenesis to cells (Tuj1, MAP2 A/B). Furthermore, Neurotrophic factors (NTF3, NGF) were increased.

FeMNP-NSCs) into the subventricular zone. 1 week later, perl's prussian blue staining (Fig. 16 a-c) and human nucleus immunostaining (Fig. 16 d-f) showed similar number of cells were settled in CC. But merged with neuronal marker Tuj1 clearly showed increased neurogenesis *in vivo* (Fig. 16 g-j,q-s, Table. 5). Other fate indicating markers (Nestin, GFAP, PDGFR) showed no significant differences (Fig. 16 j-p, t-v, Table. 5).

## 7. Blood brain barrier disruption

Evans blue dye was used to assess the permeability of the BBB. Because serum albumin cannot cross the barrier, and virtually evans blue is bound to serum albumin. In case of systemically injected evans blue is detected in brain suggest that BBB has been destroyed. In MCAo animal model (Fig. 16), BBB destruction was maximized at 24 hours (Fig. 17 d, f-h) after stroke and verified at least 72 hours (Fig. 17 e). Destruction of BBB is jeopardized, but can be used to access point to exogenous cell delivery route.

## 8. Tracking cell migrating path

We injected ZnMNP-NSCs in internal carotid artery 24 hours after initial stroke attack and forced to engraft and migrate to ischemic region by use of magnetic field. Non-invasive temporal tracking of exogenous cells by MRI, clearly showed migrating path via external capsule (EC; Fig. 18 k-l) in magnet guided group. Non guided group showed less exogenous cells in quantity and scope (Fig. 18 f-i).

In order to ensure that the MRI data fits, histological experiment was conducted. Human cytoplasm specific peroxidase staining with perl's prussian blue staining showed same cellular path with MR images (Fig. 18 e, j, o, p).

Minimum density of cells (1,000 cells/mm<sup>3</sup>) were required in order to be detected by MRI (Fig. 3 i, j). High density of cells are settled in EC (Fig. 18) in magnet guided group same as MRI. However, we found low density of exogenous cells spread-out the area of

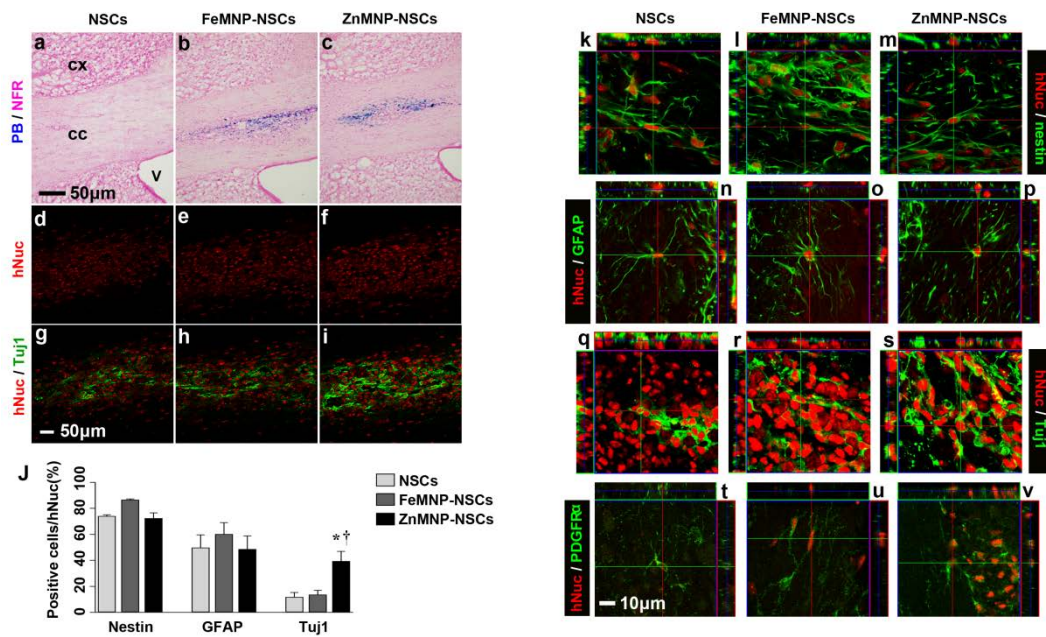


**Figure 16. Increased neuronal differentiation of ZnMNP-NSCs *in vivo*.** ZnMNP-NSCs and controls were transplanted to SVZ of the intact rat brain. (a-c), Many Prussian blue positive grafted cells were found in CC. The brain sections were counter stained with NFR. (d-f), Many hNuc-positive grafted cells (red) were detected in CC. (g-i), The number of both hNuc- and Tuj1- positive grafted cells in ZnMNP were highly increased compared to those in NSCs and FeMNP. Neural stem cell fate indicating markers were immunostained with hNuc. Nestin (k-m), GFAP (n-p), Tuj1 (q-s), PDGFR $\alpha$  (t-v). All data represent mean  $\pm$  SEM. \*  $p < 0.05$  compared to NSCs-injected group.

『**Abbreviation**』 SVZ; subventricular zone, Cx; cerebral cortex, CC; corpus callosum, V; lateral ventricle, PB; Perl's Prussian blue, NFR; nuclear fast red.

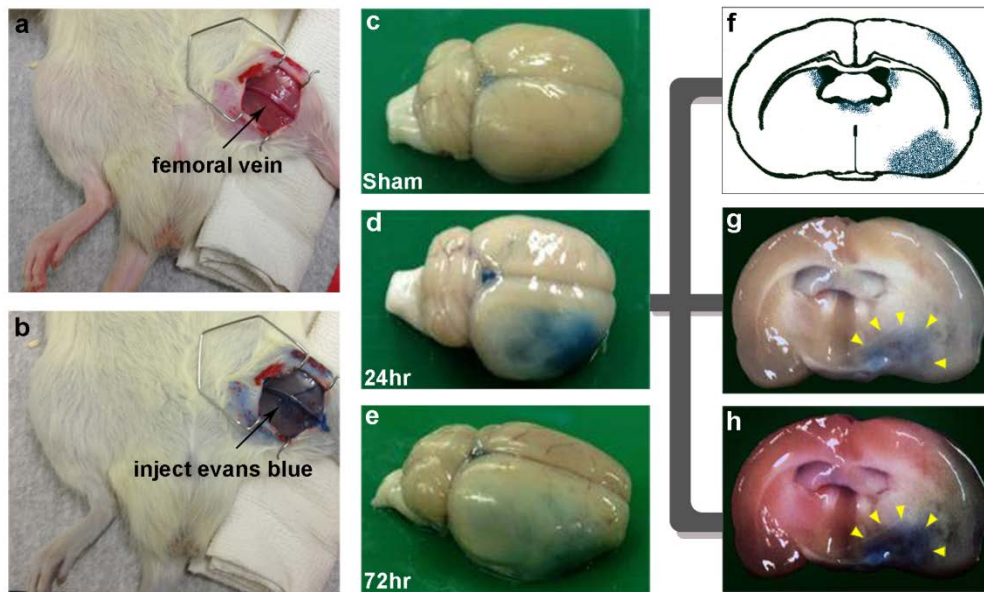


**Figure 17. Blood brain barrier disruption in stroke.** (a, b), To visualize BBB disruption in stroke brain, evans blue dye (100 mg/kg) was injected to femoral vein of adult rat. (c), There was no evans blue extravasation in normal brain tissue. (d, e) The leakage of evans blue dye was detected in the ipsilateral hemisphere to stroke at 24 hours post-infarction. A cross section of the brain at 24 hours post-infarction (f, g) and TTC staining (h) revealed the disrupted BBB area (arrowheads).

『**Abbreviation**』 BBB; blood brain barrier, TTC; 2,3,5-Triphenyltetrazolium chloride

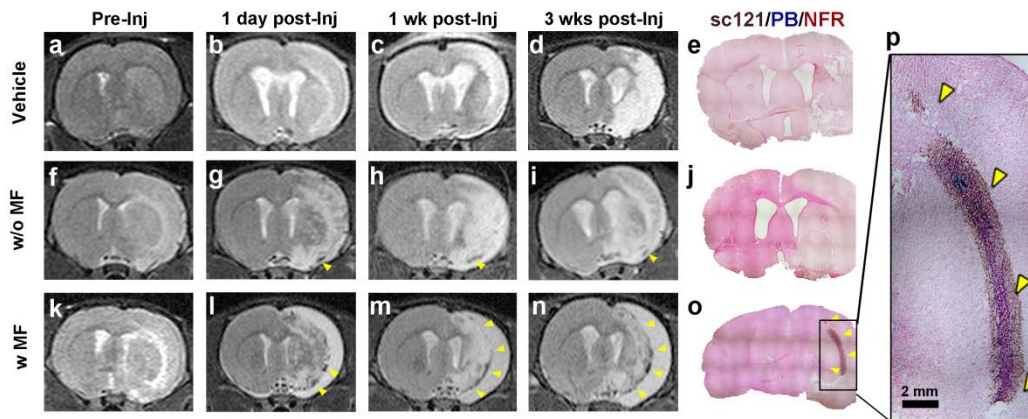


**Figure 18.** MR based *in vivo* tracking of cellular path in stroke brain. (a-d), Representative serial T2 MR brain images of vehicle injection groups. (f-i), Representative serial T2 MR brain images of ZnMNP-NSCs injection group without magnetic field. (k-n), Representative serial T2 MR brain images of ZnMNP-NSCs injection group with magnetic field. (e, j, o), human specific cytoplasm (sc121) immunostaining with Perl's prussian blue staining immediately after last MR imaging. (p), Under high magnification of (o).

『Abbreviation』 MR; magnetic resonance

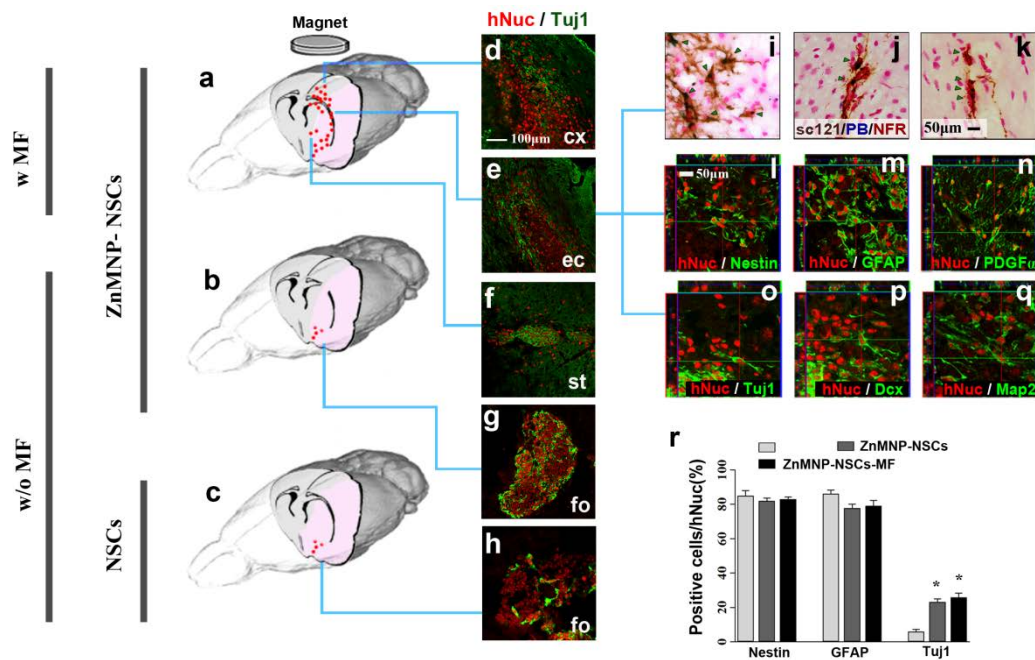


**Figure 19. In vivo histological tracking of ZnMNP-NSCs following cell injection into stroke brain.** (a), Schematic pictures showing the magnet guided migration route of injected ZnNP-NSCs. (b), Schematic pictures showing the non guided migration route of injected ZnNP-NSCs. (c), Schematic pictures showing the migration route of injected NSCs. (d-f), Magnet guided engrafted cells were settled in **cx**, **st**, **ec**. (g, h), Non guided engrafted cells were settled in fornix. (i-k), Most of labeled ZnMNP (blue, indicated by arrowhead) were remained in NSCs (brown) when analyzed at 3 weeks following cell injection. (l-q), Magnet guided engrafted cells were differentiated into multiple lineages; NSCs (l), astrocyte (m), oligodendrocyte (n), neurons (o-q). Whether magnet was presence or not, ZnMNP-NSCs were forced to neuronal differentiation (r). All data represent mean  $\pm$  SEM. \*  $p < 0.05$  compared to NSCs injected group.

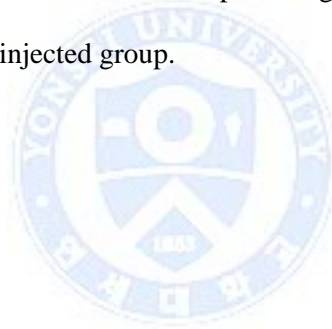
『**Abbreviation**』 cx; cerebral cortex, st; striatum, ec; external capsule

**Table 6. Differentiation pattern of Zn-doped magnetic nanoparticle-neural stem cells in stroke brain**

	NSCs	ZnMNP-NSCs	ZnMNP-NSCs-MF
<b>Nestin</b>	85.03±3.01	81.98±1.65	83.01±1.26
<b>GFAP</b>	86.26±2.09	77.85±2.29	79.14±3.12
<b>Tuj1</b>	5.96±1.36	23.24±1.74*	25.94±2.43*

All data were expressed as mean±SEM, and as a percentage of the hNuc-positive cells.

\*  $p < 0.05$  compared to NSCs injected group.





ischemic core and penumbra region including cerebral cortex and striatum (Fig. 19 d,e). These cells express human specific marker (hNuc) with neural stem cell fate specific markers (nestin, GFAP, PDGF $\alpha$ , Tuj1, Dcx, Map2; Fig. 19 l-q). As with previous studies, neuronal marker Tuj1 was increased in ZnMNP-NSCs injected group whether magnet was present or not (Fig. 19 r, Table. 6)

Next, human cytoplasm specific peroxidase staining with Perl's prussian blue staining was carried out. This image showed that ZnMNP remained in exogenous cells (Fig. 19 i-k)

## **9. Measuring engrafted cell quantities**

Some animals were given ZnMNP-Lenti-Fluc-GFP-NSCs as same as ZnMNP-NSCs. Normally, Fluc had no cellular functions, but treated with D-luciferin emitting a wave signal of near-infrared. Fluc activating signal (Photons/sec/cm<sup>2</sup>/sr) and the number of Fluc cells were directly proportional, following standard primary function curve (Fig. 2 g ;  $y=0.0238x + 297.8$ ). Therefore, engrafted cell number can be calculated by the mathematical formula. Approximately, 60 times of Fluc activity was measured in magnet guided group in 3 weeks after injection, which suggest 60 times of cells were engrafted compared to non guided cells (Fig. 20 j, Table. 7)

## **10. Therapeutic effect**

The initial brain stroke attack is resulting in serious damage. The pathogenic process leading from the initial brain stroke is getting worse, because of infarct evolution. Clearly, infarction volume in magnet guided group was not replaced. But in control groups, infarction area was steadily increased. By contrast, in magnet guided group, infarct evolution was inhibited (Fig. 21 a, Table. 8).

Assymmetric cylinder test which is designed to evaluate locomotor of CNS disorders. In MCAo animal model, impaired forelimb meant damaged brain hemisphere related fore limb function is reduced. Assymmetric cylinder test data showed improved neurological performance in magnet guided group compared to controls (Fig. 21 b, Table. 9).

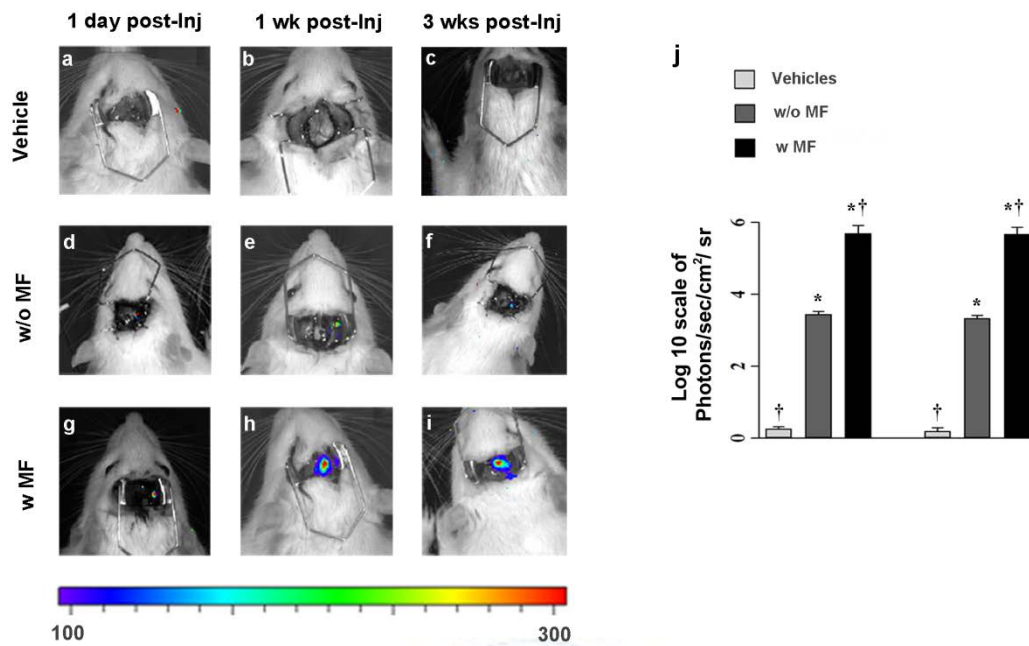


**Figure 20. Engraftment of injected cells in stroke brain.** (a-c), Vehicle injection groups showed bottom level of luciferase signals. (d-f), Luciferase signals in ZnMNP-NSCs without magnetic field group according to time intervals. (g-i), Luciferase signals in ZnMNP-NSCs with magnetic field group according to time intervals. (j), Quantitative ROI analysis that the engraftment of live cells into ischemic brain. All data represent mean  $\pm$  SEM. \*  $p < 0.05$  compared to vehicle-injected group, †  $p < 0.05$  compared to w/o MF.

**Table 7. Engraftment of magnet guided Zn-doped magnetic nanoparticle-neural stem cells in stroke brain**

	<b>Week<sup>1</sup></b>	<b>w/o MF (n=7)</b>	<b>w MF (n=8)</b>
<b>Luciferase intensity<sup>2</sup></b>	1	2,720±313.74	530,000±203,071.3*
	3	1,610±147.46	556,000±184,848.6*
<b>Common logarithm of luciferase intensity<sup>3</sup></b>	1	3.43±0.05	5.70±0.22*
	3	3.20±0.04	5.68±0.19*
<b>Assumed Cell Number<sup>4</sup></b>	1	79,800±2,290	3,930,000±1,482,420*
	3	71,800±1,076	4,120,000±1,349,394*
<b>Percentage of Cell Number<sup>5</sup></b>	1	0.26	13.10*
	3	0.24	13.73*

<sup>1</sup> Weeks after cell injection.

<sup>2</sup> Fluc signal intensity, Photons/sec/cm<sup>2</sup>/sr.

<sup>3</sup> Log10 scale of Fluc signal intensity.

<sup>4</sup> Assumed cell number based on standard curve.

<sup>5</sup> Assumed cell number as a percentage of total injected cell number.

All data were expressed as mean±SEM. \*  $p < 0.05$  compared to w/o MF.

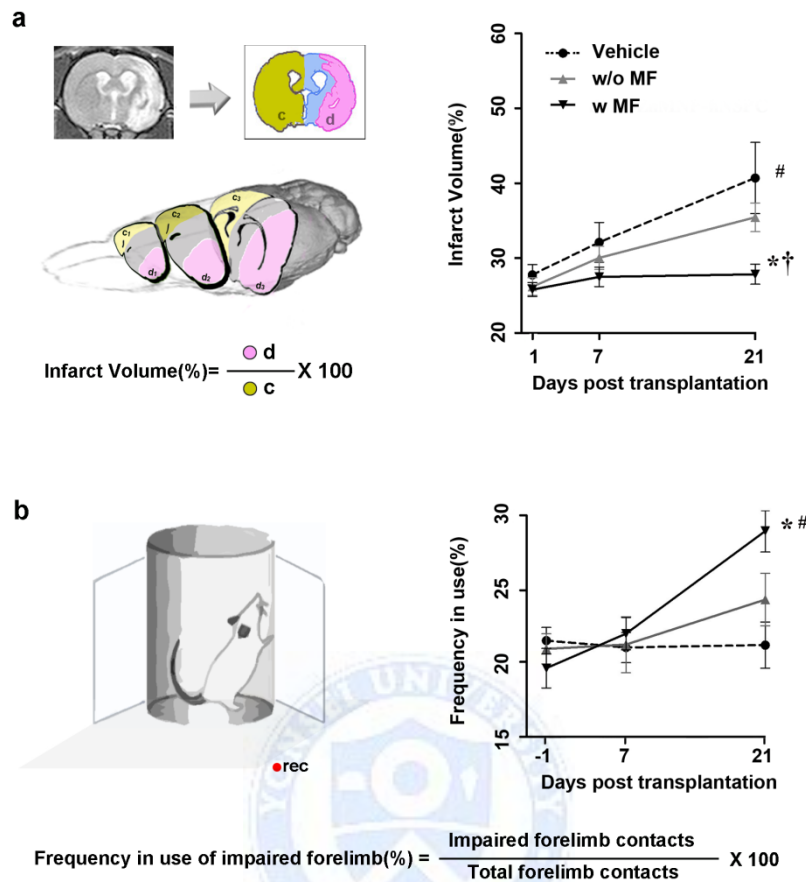


**Figure 21. Therapeutic potentials of magnetically guided ZnMNP-NSCs in ischemic brain.** (a), Cerebral infarct volume was significantly reduced in the magnet-guided group compared to the non-magnet-guided (w/o MF) or vehicle-injected group at 3 weeks following injection. (b), Asymmetric cylinder test showed the significant improved motor performance in the magnet-guided cell group (w MF) at 3 weeks following cell injection to stroke brain compared to vehicle-injected group. (c), Area of contralateral cerebral hemisphere. (d), Area of infarct in the ipsilateral hemisphere to stroke. All data represent mean  $\pm$  SEM. \*  $p < 0.05$  compared to vehicle-injected group,  $^\dagger p < 0.05$  compared to w/o MF. #  $p < 0.05$  compared to the first collected data in the same group.

**Table 8. Infarction volume measurement**

<b>Day<sup>1</sup></b>	<b>Vehicle (n=8)</b>	<b>w/o MF (n=18)</b>	<b>w MF (n=9)</b>
<b>1</b>	27.72±1.37	26.18±1.17	25.79±0.94
<b>7</b>	32.11±2.65	30.03±1.55	27.48±1.30
<b>21</b>	40.71±4.75 <sup>#</sup>	35.45±1.92	27.85±1.33 <sup>*†</sup>
<b>Rate<sup>2</sup></b>	1.43±0.09	1.36±0.67	1.08±0.04 <sup>*†</sup>

<sup>1</sup> Days after cell injection.

<sup>2</sup> Increasing rate of infarction at Day21 measurement as a percentage of Day1 measurement.

All data were expressed as mean±SEM. \*  $p < 0.05$  compared to vehicle-injected group, <sup>†</sup>  $p < 0.05$  compared to w/o MF, #  $p < 0.05$  compared to the first collected data in the same group.

**Table 9. Assymmetric neurological cylinder test**

<b>Day<sup>1</sup></b>	<b>Vehicle (n=8)</b>	<b>w/o MF (n=17)</b>	<b>w MF (n=9)</b>
<b>1</b>	21.64±0.89	26.64±0.90	19.80±1.32
<b>7</b>	21.18±1.01	21.86±1.43	22.11±1.08
<b>21</b>	21.34±1.54	23.33±1.31	28.96±1.41 <sup>*#</sup>

<sup>1</sup> Days after cell injection.

All data were expressed as mean±SEM. \*  $p < 0.05$  compared to vehicle-injected group. #  $p < 0.05$  compared to the first collected data in the same group.



#### IV. DISCUSSION

Over the past decades, medical breakthroughs had improved the survival rate of brain stroke attack. Blood supplies were restored by use of recombinant tissue plasminogen activator (rt-PA) or antiplatelet medicines. Nevertheless, survivals suffered by impairment of sensation, movement or cognition because the damaged brain tissue has short ability of restoration.

The brain continues to produce new cells throughout life and these appear to be capable of taking on normal functions. However, brain cannot produce sufficient amount of cells in the injury of brain including ischemia. Therefore, we should fill in the insufficient production of new cells generated by exogenous neural stem cells. But transplanted neural stem cells cannot produce enough new neurons and cannot secure cell viability likewise endogenous cellular source, because of the harsh biological microenvironments in areas of pathology. Researchers attempts to overcome such limitations, NSCs were transplanted far apart from those target lesions but chemoattractive mechanisms were limited owing to complicated chemoattractive mechanisms.

As an alternative solution to the chemotaxis, magnetotaxis is an effective cell manipulating method. ZnMNP gave rise magnetotactic ability to neural stem cells. ZnMNP-NSCs were capable of migration toward to magnet  $12\mu\text{m}/\text{hour}$  in intact brain. Systemically injected magnetotactic NSCs through carotid artery and guided by magnet can expect a similar delivery efficiency of intracerebral cell transplantation in live animal while avoiding invasive craniectomy. In addition, ZnMNP did not alter cell proliferation, cytotoxicity and neurosphere morphology.

Unexpectedly, in genetic screening by use of traditional PCR, we found different gene expressing pattern. Proneural transcription factors and neuronal gene expression level were increased. Same results came out from

immunocytochemistry, Q-PCR, western blotting, and immuno histochemistry. Through the wnt signaling antagonist DKK1 treating, we realized the involvement of wnt signaling pathway. WNT signaling has a crucial role in early development through the regulation of cell fate decision, cell movement and tissue polarization.<sup>59,60</sup> In the central nervous system, Wnt signaling has been implicated in the neurogenesis, axon remodeling, dendrite and synapse formation. In xenopus system, zinc finger transcription factor ZIC family were known as wnt signaling pathway activator. We found *ZIC1* and *ZIC2* increment in ZnMNP-NSCs, while *ZIC3*, *ZIC4*, *ZIC5* reveal no difference. Wnt reporting gene, *AXIN2* was increased, either. There were several strong evidences of wnt signaling involvement ; DKK1, Wnt ligands, ZIC transcription factors,  $\beta$ -catenin.

In addition, ZnMNP showed augmented of NGF, NTF3 secretion compared to controls. NGF is a representative neurotrophic factor known as the function of survival of neurons.<sup>61,62</sup> NTF3 is known as not only neurotrophic effects but also immunomodulatory factor.<sup>61,63</sup>

We found ZIC transcription factors between ZnMNP and wnt signaling pathway. In xenopus system, *Zic1* is an activator of wnt signaling pathway.<sup>64</sup> However, we did not find the relation between ZnMNP and ZIC transcription factors. Possible mechanisms are Zn ion concentrations but Zn ion concentration showed no significant changes in ZnMNP-NSCs (Fig. 5). One reason for this assumption is the lack of zinc ion inhibit the neurogenesis and brain formation.<sup>24,25</sup> For now, less than the ion level that can be detected, may activate the ZIC transcription factors.

Brain ischemia is accompanied by the destruction of the BBB.<sup>40</sup> Destruction of BBB is jeopardized, but can be used to access point to exogenous cells. Therefore, we injected ZnMNP-NSCs in internal carotid artery. Magnet guided injected cells were concentrated to BBB destructed area and penetrated into the brain and spread to ischemic core and penumbra area.



Therapeutic effect of NSCs vary depending on the number of cells at areas of pathology. Magnet guided cell delivery methods revealed 60 times effective delivery (Table. 6) rate than non-guided cell injection group. As a result, therapeutic effects of magnet guided group were better than non-guided group in infarct volume measurement and neurological cylinder test (Fig. 21, Table. 8, Table. 9).

ZnMNP promote NSCs neurogenesis in a stepwise process (Fig. 15) and give rise to superparamagnetic ability to NSCs (Fig. 6-7). Both features synergize the therapeutic effect of stroke brain. It was reported that grafted NSCs derived neurons exhibit synaptic integration into host neural circuitries.<sup>9,41</sup> Our data show increased neurogenesis through wnt signaling pathway (Fig. 12-15), suggesting that neuronal replacement may contributed to improvement. Superparamagnetic features enhance the number of grafted NSCs and NSCs-derived neurons (Fig. 20, Table. 6, Table. 7). Indeed, this property facilitates MRI based cell tracking.

NSCs secrete several neurotrophic factors such as NGF, NTF3, NTF4, GDNF, BDNF.<sup>65</sup> Western blot analysis reveal increased secretion of NGF and NTF3 in ZnMNP-NSCs compared to controls (Fig. 14). Some reports NGF secretion was related to Wnt3a<sup>62,65</sup> and NTF-3 secretion was related to Wnt1.<sup>63,65</sup> These data indicate that ZnMNP-NSCs provide large amount of NFG and NFT3 to ischemic brain. NTF4, BDNF, GDNF secretion level showed no difference among all groups *in vitro*, but based on the number of engrafted cells, we assumed that NTF4, BDNF, GDNF were also provided large quantities to ischemic brain.

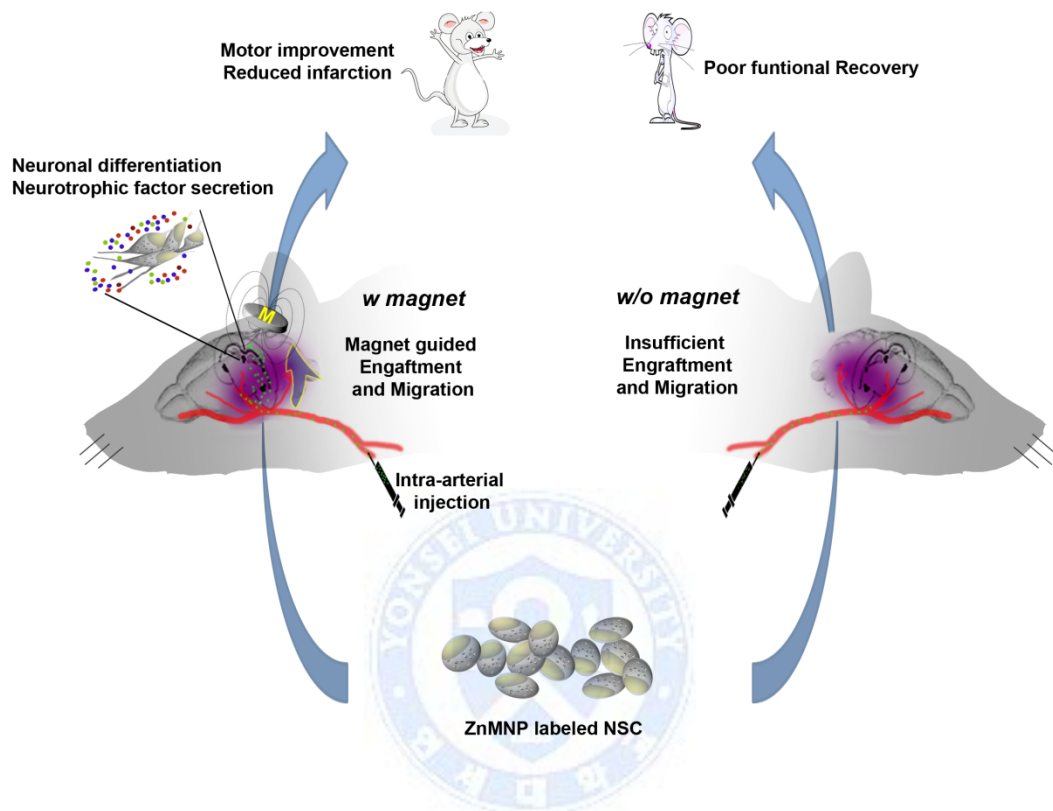


**Figure 22. Magnetic nanoparticles control neural stem cell behavior in ischemic stroke.** ZnMNP-labeled NSCs are non-invasively injected via the internal carotid artery to rat stroke brain. In the presence of external magnetic field, ZnMNP-NSCs exhibit the specific migration toward the ischemic regions, robust engraftment within the injured regions, and neuronal differentiation which replace damaged neurons and secrete neuroprotective factors. Consequently, animals show the decreased cerebral infarct volume and improved of motor function. In contrast, injected NSCs exhibit poor *in vivo* control of migration, engraftment and differentiation which subsequently show little therapeutic benefits.

## V. CONCLUSION

This study showed several improvement compared to traditional stem cell therapies. First, cells are capable of magnet guided delivery to ischemic region. It enables effective cell delivery to central nervous system without craniectomy. This magnetotactic delivery is superior to chemotactic delivery. Magnetotactic delivery required no genetic nor chemical injections and easy to remove. Second, cell delivery process and monitoring process were minimally-invasive. By use of MRI, cellular location were traced in real time and at the same time, pathologic process could be monitored. Third, wnt signaling mediated neurogenesis is occurred without any genetic modifications nor biochemical treatment. Consequently, we remote control of NSCs migration, engraftment, neurogenesis and tracking *in vivo* by use of superparamagnetic nanoparticle and static magnetic field. This research is applicable to other neurological disorders such as traumatic brain injury, hypoxia ischemic injury and spinal cord injury.

ZnMNP has tremendous possibilities. This particle can be combined with various of biochemical molecules such as DNA, RNA, proteins and easily transfected to cells and no cytotoxicity. Traditional delivery methods such as viral delivery, electroporated delivery, liposome based methods have the limits. Viral delivery showed high efficiency but did not deviated from the arguing about safety issues. Viral materials caused immune-reponse or cancer by random genetic manipulation. In 1999, Jesse Gelsinger, 18 years old, suffered from ornithine transcarbamylase deficiency, was died in a phase I clinical trial for gene therapy using adenoviral vector by the University of Pennsylvania.<sup>66</sup> In 2000, One SCID patient took the leukemia during the clinical trial for gene therapy in France.<sup>66</sup> By contrast, non viral delivery methods are secured about safety issues but gene delivery efficiency is not good. ZnMNP transfection shows the efficiency of 95% (Fig. 4 e). By using ZnMNP as a gene delivery vector, both delivery efficiency and safety are secured.

NSCs possess various therapeutic potentials. NSCs can migrate to desired area, generate new neurons or glial cells, replace damaged cells. In addition, therapeutic neurotrophic factors such as NGF, NTF3, NTF4, BDNF, GDNF, VEGF and FGF are secreted by NSCs. Besides, several anti-inflammatory molecules are originated from NSCs. Applying the gene delivery ability of ZnMNP's to NSCs, various genetic modified therapeutic NSCs will be presented to the treatment of various diseases.



## REFERENCES

1. Iadecola C, Anrather J. Stroke research at a crossroad: asking the brain for directions. *Nat Neurosci* 2011;14:1363-8.
2. Hossmann KA. Pathophysiology and therapy of experimental stroke. *Cell Mol Neurobiol* 2006;26:1057-83.
3. Murphy TH, Corbett D. Plasticity during stroke recovery: from synapse to behaviour. *Nat Rev Neurosci* 2009;10:861-72.
4. Kent TA, Shah SD, Mandava P. Improving early clinical trial phase identification of promising therapeutics. *Neurology* 2015;85:274-83.
5. Temple S. The development of neural stem cells. *Nature* 2001;414:112-7.
6. Ming GL, Song H. Adult neurogenesis in the mammalian brain: significant answers and significant questions. *Neuron* 2011;70:687-702.
7. Breunig JJ, Haydar TF, Rakic P. Neural stem cells: historical perspective and future prospects. *Neuron* 2011;70:614-25.
8. R Z, Z Z, L W, Y W, A G, L Z, et al. Activated neural stem cells contribute to stroke-induced neurogenesis and neuroblast migration toward the infarct boundary in adult rats. *Journal of cerebral blood flow & metabolism* 2004;24:441-8.
9. Mine Y, Tatarishvili J, Oki K, Monni E, Kokaia Z, Lindvall O. Grafted human neural stem cells enhance several steps of endogenous neurogenesis and improve behavioral recovery after middle cerebral artery occlusion in rats. *Neurobiol Dis* 2013;52:191-203.
10. Imitola J, Raddassi K, Park KI, Mueller FJ, Nieto M, Teng YD, et al. Directed migration of neural stem cells to sites of CNS injury by the stromal cell-derived factor 1alpha/CXC chemokine receptor 4 pathway. *Proc Natl Acad Sci U S A* 2004;101:18117-22.
11. Park KI, Teng YD, Snyder EY. The injured brain interacts reciprocally with neural stem cells supported by scaffolds to reconstitute lost tissue. *Nat Biotechnol* 2002;20:1111-7.
12. Xue L, Wang J, Wang W, Yang Z, Hu Z, Hu M, et al. The effect of stromal cell-derived factor 1 in the migration of neural stem cells. *Cell Biochem Biophys* 2014;70:1609-16.
13. Yoshinaga T, Hashimoto E, Ukai W, Ishii T, Shirasaka T, Kigawa Y, et al. Effects of atelocollagen on neural stem cell function and its migrating capacity into brain in psychiatric disease model. *J Neural Transm* 2013;120:1491-8.
14. Jang JT, Nah H, Lee JH, Moon SH, Kim MG, Cheon J. Critical enhancements of MRI contrast and hyperthermic effects by dopant-controlled magnetic nanoparticles. *Angew Chem Int Ed Engl* 2009;48:1234-8.
15. Estelrich J, Escribano E, Queralt J, Busquets MA. Iron oxide nanoparticles

- for magnetically-guided and magnetically-responsive drug delivery. *Int J Mol Sci* 2015;16:8070-101.
16. Na HB, Song IC, Hyeon T. Inorganic Nanoparticles for MRI Contrast Agents. *Advanced Materials* 2009;21:2133-48.
  17. Guzman R, Uchida N, Bliss TM, He D, Christopherson KK, Stellwagen D, et al. Long-term monitoring of transplanted human neural stem cells in developmental and pathological contexts with MRI. *Proc Natl Acad Sci U S A* 2007;104:10211-6.
  18. Daadi MM, Li Z, Arac A, Grueter BA, Sofilos M, Malenka RC, et al. Molecular and magnetic resonance imaging of human embryonic stem cell-derived neural stem cell grafts in ischemic rat brain. *Mol Ther* 2009;17:1282-91.
  19. Kim HT, Kim IS, Lee IS, Lee JP, Snyder EY, Park KI. Human neurospheres derived from the fetal central nervous system are regionally and temporally specified but are not committed. *Exp Neurol* 2006;199:222-35.
  20. Subramanian S, Srienc F. Quantitative analysis of transient gene expression in mammalian cells using the green fluorescent protein. *Journal of biotechnology* 1996;49:137-51.
  21. Arbab AS, Hashaw LA, Miller BR, Jordan EK, Lewis BK, Kalish H, et al. Characterization of biophysical and metabolic properties of cells labeled with superparamagnetic iron oxide nanoparticles and transfection agent for cellular MR imaging. *Radiology* 2003;229:838-46.
  22. Bravman JC, Sinclair R. The preparation of cross-section specimens for transmission electron microscopy. *Journal of electron microscopy* 1984;1:53-61.
  23. Muylle FA, Adriaensen D, De Coen W, Timmermans JP, Blust R. Tracing of labile zinc in live fish hepatocytes using FluoZin-3. *Biometals* 2006;19:437-50.
  24. Wolford JL, Chishti Y, Jin Q, Ward J, Chen L, Vogt S, et al. Loss of Pluripotency in Human Embryonic Stem Cells Directly Correlates with an Increase in Nuclear Zinc. *Plos One* 2010;5:e12308.
  25. Fukada T, Yamasaki S, Nishida K, Murakami M, Hirano T. Zinc homeostasis and signaling in health and diseases: Zinc signaling. *J Biol Inorg Chem* 2011;16:1123-34.
  26. Wiggins H, Rappoport J. An agarose spot assay for chemotactic invasion. *Biotechniques* 2010;48:121-4.
  27. Chen Z-J, Broaddus WC, Viswanathan RR, Raghavan R, Gillies GT. Intraparenchymal drug delivery via positive-pressure infusion: experimental and modeling studies of poroelasticity in brain phantom gels. *IEEE transactions of biomedical engineering* 2002;49:85-96.
  28. Porter AG, Janicke RU. Emerging roles of caspase-3 in apoptosis. *Cell Death Differ* 1999;6:99-104.

29. Negoescu A, Lorimier P, Labat-Moleur F, Drouet C, Robert C, Guillertmet C, et al. In situ apoptotic cell labeling by the TUNEL method: improvement and evaluation on cell preparations. *The journal of histochemistry and cytochemistry* 1996;44:959-68.
30. Kang MA, So EY, Simons AL, Spitz DR, Ouchi T. DNA damage induces reactive oxygen species generation through the H2AX-Nox1/Rac1 pathway. *Cell Death Dis* 2012;3:e249.
31. Olive PL, Banath JP. The comet assay: a method to measure DNA damage in individual cells. *Nat Protoc* 2006;1:23-9.
32. Roy NS, Wang S, Jiang L, Kang J, Benraiss A, Harrison-Restelli C, et al. In vitro neurogenesis by progenitor cells isolated from the adult human hippocampus. *Mature medicine* 2000;6:271-7.
33. Bisson I, Prowse DM. WNT signaling regulates self-renewal and differentiation of prostate cancer cells with stem cell characteristics. *Cell Res* 2009;19:683-97.
34. Kuwabara T, Hsieh J, Muotri A, Yeo G, Warashina M, Lie DC, et al. Wnt-mediated activation of NeuroD1 and retro-elements during adult neurogenesis. *Nat Neurosci* 2009;12:1097-105.
35. Lee IS, Jung K, Kim IS, Park KI. Amyloid-beta oligomers regulate the properties of human neural stem cells through GSK-3beta signaling. *Exp Mol Med* 2013;45:e60.
36. Lee H, Yun S, Kim IS, Lee IS, Shin JE, Park SC, et al. Human fetal brain-derived neural stem/progenitor cells grafted into the adult epileptic brain restrain seizures in rat models of temporal lobe epilepsy. *PLoS One* 2014;9:e104092.
37. Popp A, Jaenisch N, Witte OW, Frahm C. Identification of oschemic regions in a rat model of stroke. *Plos one* 2009;4:e4764.
38. Aspey BS, Taypor FL, Terruli M, Harrison MJG. Temporary middle cerebral artery occlusion in the rat: consistent protocol for a model of stroke and reperfusion. *Neuropathology and applied neurology* 2000;25:232-42.
39. Longa E, Weinstein P, Carlson S, Cimmins R. Reversible middle cerebral artery occlusion without craniectomy in rats. *Stroke* 1989;20:84-91.
40. Yan J, Zhou B, Taheri S, Shi H. Differential Effects of HIF-1 inhibition by YC-1 on the overall outcome and blood-brain barrier damage in a rat model of ischemic stroke. *Plos One* 2011;6:e27798.
41. Kelly S, Bliss TM, Shah AK, Sun GH, Ma M, Foo WC, et al. Transplanted human fetal neural stem cells survive, migrate, and differentiate in ischemic rat cerebral cortex. *Proc Natl Acad Sci U S A* 2004;101:11839-44.
42. Osanai T, Kuroda S, Sugiyama T, Kawabori M, Ito M, Shichinohe H, et al. Therapeutic effects of intra-arterial delivery of bone marrow stromal cells in traumatic brain injury of rats--in vivo cell tracking study by near-

- infrared fluorescence imaging. *Neurosurgery* 2012;70:435-44; discussion 44.
43. Chua JY, Pendharkar AV, Wang N, Choi R, Andres RH, Gaeta X, et al. Intra-arterial injection of neural stem cells using a microneedle technique does not cause microembolic strokes. *J Cereb Blood Flow Metab* 2011;31:1263-71.
  44. Shin T-h, Choi J-s, Yun S, Kim I-S, Song H-T, Kim Y, et al. T1 and T2 dual-mode MRI contrast agent for enhancing accuracy by engineered nanomaterials. *ACS nano* 2014;8:3393-401.
  45. Tatlisumak T, Takano K, Carano RAD, Miller LP, Foster AC, Fisher M, et al. Delayed Treatment With an Adenosine Kinase Inhibitor, GP683, Attenuates Infarct Size in Rats With Temporary Middle Cerebral Artery Occlusion Editorial Comment. *Stroke* 1998;29:1952-8.
  46. Pendharkar AV, Chua JY, Andres RH, Wang N, Gaeta X, Wang H, et al. Biodistribution of neural stem cells after intravascular therapy for hypoxic-ischemia. *Stroke* 2010;41:2064-70.
  47. Hicks A, Schallert T, Jolkkonen J. Cell-based therapies and functional outcome in experimental stroke. *Cell Stem Cell* 2009;5:139-40.
  48. Brooks SP, Dunnett SB. Tests to assess motor phenotype in mice: a user's guide. *Nat Rev Neurosci* 2009;10:519-29.
  49. Conti L, Cattaneo E. Neural stem cell systems: physiological players or in vitro entities? *Nat Rev Neurosci* 2010;11:176-87.
  50. Kriegstein A, Alvarez-Buylla A. The glial nature of embryonic and adult neural stem cells. *Annu Rev Neurosci* 2009;32:149-84.
  51. Svendsen CN, Borg MGt, Armstrong RJE, Rosser AE, Chandran S, Ostensfeld T, et al. A new method for the rapid and long term growth of human neural precursor cells. *Journal of neuroscience methods* 1998;85:141-52.
  52. Ferreira L, Karp JM, Nobre L, Langer R. New opportunities: the use of nanotechnologies to manipulate and track stem cells. *Cell Stem Cell* 2008;3:136-46.
  53. Pankhurst QA, Thanh NTK, Jones SK, Dobson J. Progress in applications of magnetic nanoparticles in biomedicine. *Journal of Physics D: Applied Physics* 2009;42:224001.
  54. Kolosnjaj-Tabi J, Wilhelm C, Clement O, Gazeau F. Cell labeling with magnetic nanoparticles: opportunity for magnetic cell imaging and cell manipulation. *J Nanobiotechnology* 2013;11 Suppl 1:S7.
  55. Song M, Kim Y-J, Kim Y-h, Roh J, Kim SU, Yoon B-W. Using a neodymium magnet to target delivery of ferumoxide-labeled human neural stem cells in a rat model of focal cerebral ischemia. *Human gene therapy* 2010;21:603-10.
  56. Shen H, Tong S, Bao G, Wang B. Structural responses of cells to intracellular magnetic force induced by superparamagnetic iron oxide nanoparticles. *Phys. Chem. Chem. Phys* 2014;16:1914-20.



57. Shin J, Lee K-M, Lee JH, Lee J, Cha M. Magnetic manipulation of bacterial magnetic nanoparticle-loaded neurospheres. *Integr. Biol* 2014;6:532-9.
58. Lledo PM, Alonso M, Grubb MS. Adult neurogenesis and functional plasticity in neuronal circuits. *Nat Rev Neurosci* 2006;7:179-93.
59. Marchetti B, Pluchino S. Wnt your brain be inflamed? Yes, it Wnt! *Trends Mol Med* 2013;19:144-56.
60. Valenta T, Hausmann G, Basler K. The many faces and functions of beta-catenin. *EMBO J* 2012;31:2714-36.
61. Kokaia Z, Martino G, Schwartz M, Lindvall O. Cross-talk between neural stem cells and immune cells: the key to better brain repair? *Nat Neurosci* 2012;15:1078-87.
62. TC W, DC R, P K, HV N, KY P, G N, et al. Promoter-activated expression of nerve growth factor for treatment of neurodegenerative diseases. *Gene therapy* 1999;6:1648-60.
63. Yang J, Yan Y, Xia Y, Kang T, Li X, Ciric B, et al. Neurotrophin 3 transduction augments remyelinating and immunomodulatory capacity of neural stem cells. *Mol Ther* 2014;22:440-50.
64. Merzdorf CS, Sive HL. The *zic1* gene is an activator of Wnt signaling. *Int J Dev Biol* 2006;50:611-7.
65. Drago D, Cossetti C, Iraci N, Gaude E, Musco G, Bachi A, et al. The stem cell secretome and its role in brain repair. *Biochimie* 2013;95:2271-85.
66. Abeel S. Smoke and mirrors; Jesse Gelsinger, human experimentation, and gene therapy. *International journal of the humanities* 2010;8:15-30.

ABSTRACT (IN KOREAN)

자성나노입자를 통한 신경줄기세포의 뇌내 제어조절

<지도교수 박 국 인>

연세대학교 대학원 의과학과

윤 석 환

지난 20여 년간의 연구를 통하여 한 번 손상되면 재생되지 않는 것으로 알려져 있는 포유류의 중추신경계에 내인성 신경줄기세포의 존재가 밝혀졌다. 신경줄기세포는 미분화된 상태로 계속 증식하는 자가갱신을 보이고, 다양한 신경원세포 및 교세포로 분화하는 특성을 보이므로, 뇌졸중을 비롯한 중추신경계 질환 치료에 적용할 경우, 사멸한 신경세포를 대체하고, 손상된 신경회로를 재건하여 신경재생을 유도하는 가능성을 보인다. 그럼에도 불구하고, 신경줄기세포 이식치료시 손상된 신경부위로의 이주 및 생착, 손상된 신경세포 부위에서의 신생 신경세포생성을 제어할 수 없어 치료적 유용성은 제한적이다.

최근 나노기술은 세포를 제어 및 조절 가능한 수준으로 발달하고 있으며, 탄소나노튜브나 나노형광물질, 자성나노입자가 이미 줄기세포의 추적, 분화 및 이식 연구에 활발하게 사용되고 있다.

본 연구에서는 초고감도 자성나노입자를 신경줄기세포에 도입하여, 외부 자기장에 의해서 생체 내 신경줄기세포의 위치를 제어/조절 할 수 있고, MRI에 의해 세포의 위치를 추적할 수 있으며, Wnt 신호전달 기작에 의해서 신경원세포로 분화가 가능하도록 하였다. 상기의 신경줄기세포를 뇌졸중 동물 모델의 경동맥에 주입하고 외부 자기장에 노출시켰을 때, 주입된 세포는 손상된 뇌조직으로 효과적으로 이주 및 생착하였고, 신경원세포로 분화하고, 신경영양인자를 뇌손상 조직에 공급하여 뇌손상 용적의 증가를 억제하였으며, 신경행동의 개선을 보였다.

---

핵심되는 말 : 자성나노입자, 신경줄기세포, 뇌졸중, 세포치료, 주자성